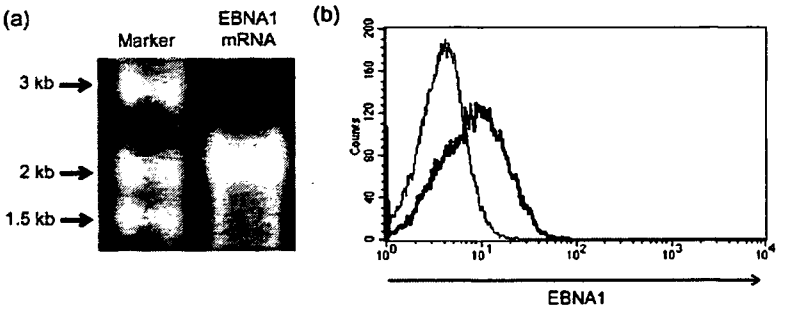

Fig. 1. EBNA1 expression in cells transfected with *in vitro*-transcribed full-length mRNA. (a) *In vitro*-transcribed full-length EBNA1 mRNA produced successfully from an EBNA1-cDNA plasmid. The quality of the EBNA1 mRNA was assessed by gel electrophoresis followed by staining with ethidium bromide. (b) EBNA1 protein expression in EBNA1 mRNA-transfected CD40-B cells. CD40-B cells were transfected with full-length EBNA1 mRNA by electroporation and intracellular staining of EBNA1 protein was performed and analysed by flow cytometry.

the amount of mRNA was sufficient and seen as a single band on the gel (Fig. 1a). Transfection was then performed by electroporation and EBNA1 expression was detected in most CD40-B cells, although the mean fluorescent intensity appeared to be low (Fig. 1b).

Induction of EBNA1-specific CTL lines and clones by using EBNA1 mRNA-transfected APCs

To explore the capacity for T-cell stimulation, autologous $CD8^+$ T lymphocytes were co-cultured with CD40-B cells transfected with full-length EBNA1 mRNA, and IFN-γ-producing cells were enumerated by ELISPOT assay. As shown in Fig. 2(a), $CD8^+$ T lymphocytes of donor Y01 produced IFN-γ spots without *in vitro* stimulation. As $CD8^+$ T lymphocytes of other donors did not produce significant spots on *ex vivo* analysis, the T cells were stimulated weekly with irradiated CD40-B cells that had been transfected with the full-length EBNA1 mRNA. After two rounds of stimulation, $CD8^+$ T lymphocytes of another donor (K04) produced IFN-γ spots upon contact with autologous CD40-B cells transduced with EBNA1 mRNA in the ELISPOT assay (Fig. 2a). These data indicate that the full-length EBNA1 mRNA was translated and that $CD8^+$ T-lymphocyte epitopes are processed and presented on APCs.

Next, EBNA1-specific CTL clones were established by using donor Y01 monocyte-derived DCs transfected with full-length EBNA1 mRNA. The transduced DCs were distributed in 96-well plates and used to stimulate autologous $CD8^+$ T lymphocytes in the presence of IL-7 and IL-12. After three rounds of stimulation, aliquots of each microculture were tested for their ability to secrete IFN-γ specifically upon contact with autologous CD40-B cells transduced with EBNA1 mRNA in the ELISPOT assay. Thirty-two microcultures out of 36 wells were scored as EBNA1-specific (data not shown), and lymphocytes from two well-growing microcultures were cloned by limiting dilution. CTL clones B5 and C6 were thus established, recognizing EBNA1 mRNA-transfected autologous CD40-B cells and autologous LCLs, but not mock-transfected autologous CD40-B cells or HLA-mismatched allogeneic LCLs (Fig. 2).

Identification of the presenting HLA molecules

The donor was typed genetically as HLA-A*2402, -A*3101, -B*1507, -B*3501 and -Cw*0303. To identify the antigen-presenting HLA molecule, a panel of partially HLA-matched LCLs was used to stimulate clones B5 or C6 to produce IFN-γ. In addition to autologous LCLs, allogeneic LCLs expressing HLA-B*3501 were recognized by CTL clone C6 (Fig. 3a), and one LCL with HLA-Cw*0303 and one with -Cw*0304 were recognized by clone B5 (Fig. 3b), demonstrating that HLA-B*3501 is the putative restriction element for clone C6 recognition, whilst both HLA-Cw*0303 and -Cw*0304 act for clone B5.

Identification of EBNA1 antigenic peptides

To identify the epitope region, clones B5 and C6 were stimulated with autologous CD40-B cells incubated with sets of peptides of 20 aa length, overlapping by 13 aa and covering the complete EBNA1 protein sequence without GAr. Because the primary structure of GAr is not likely to be contained in MHC class I epitopes, we did not include this part as an epitope source. Peptide 24 was recognized by clone C6 (Fig. 4). Regarding the HLA-B*3501-restricted epitope, HPVGEADYFEY has been reported previously (Blake *et al.*, 1997). As this epitope sequence is located in the centre of peptide 24 (aa 402–421) (Fig. 5a), we tested whether clone C6 might recognize HPVGEADYFEY-pulsed autologous CD40-B cells and confirmed a response to HPVGEADYFEY-pulsed stimulation (data not shown).

In the case of clone B5, two overlapping peptides, 38 (aa 500–519) and 39 (aa 507–526), were recognized (Fig. 4), sharing the 13 aa sequence VFVYGGSKTSLYN [underlined in Fig. 5(b)]. To predict the optimal epitope binding to HLA-Cw*0303, the program SYFPEITHI was applied. Because the anchor leucine at the C terminus and the auxiliary anchors valine and tyrosine at the third position of epitopes were predicted by the program, we examined the 11mer (VFVYGGSKTSL) and the 10mer (FVYGGSKTSL) (Fig. 5b). Half-maximal recognition of the peptide-pulsed target cells was obtained with 5–10 nM of the 10mer peptide and 1–5 nM of the 11mer (Fig. 5c), suggesting that these two peptides may be the optimal epitopes. The 9mer,

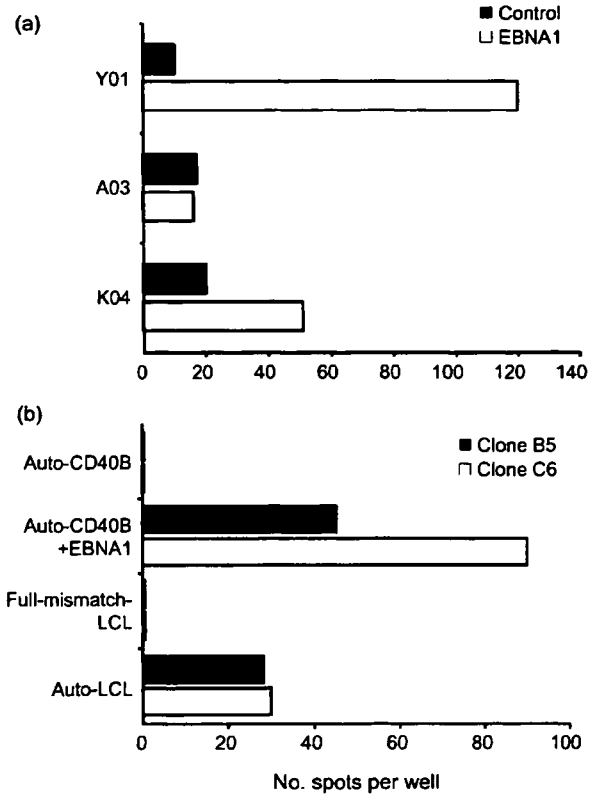

Fig. 2. Presence of anti-EBNA1 T cells in cultures primed with EBNA1 mRNA-transfected APCs. (a) Numbers of IFN-γ-producing cells from $CD8^+$ T lymphocytes without *in vitro* stimulation (Y01) or after two rounds of stimulation (A03 and K04) in ELISPOT assays. Aliquots of 100000 cells were cultured in single wells with autologous CD40-B cells transduced with full-length EBNA1 mRNA for 20 h. Data from one representative experiment of two are shown. (b) $CD8^+$ T cells from one selected donor were stimulated with autologous DCs transfected with *in vitro*-transcribed EBNA1 mRNA. After three stimulations at weekly intervals, polyclonal $CD8^+$ T cells from two positive cultures were cloned by limiting dilution. Established clones B5 and C6 were then tested for recognition of EBNA1 mRNA-transfected autologous CD40-B cells and autologous LCLs by ELISPOT assay. Five thousand CTLs were seeded in each well. Data from one representative experiment of two are shown.

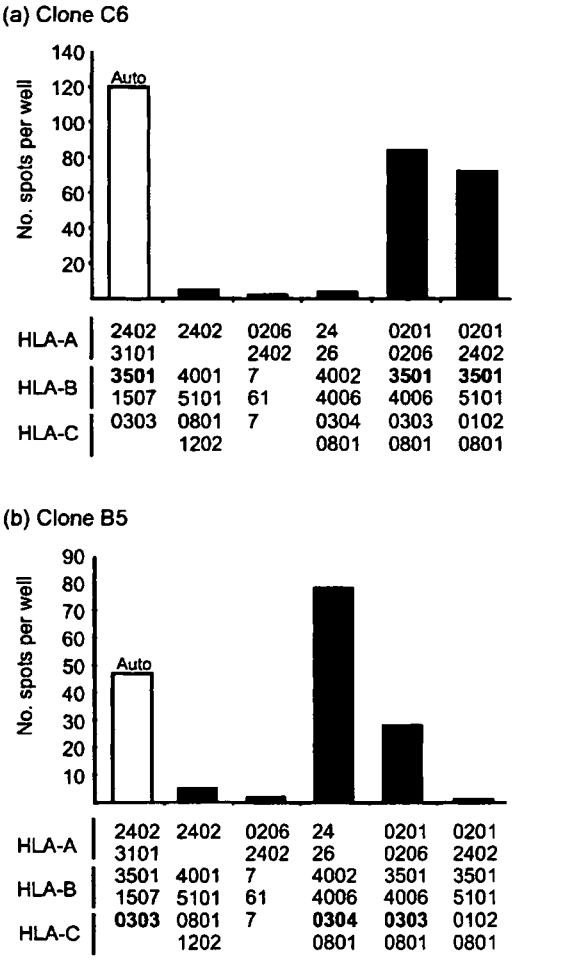

Fig. 3. Identification of presenting HLA molecules for EBNA1-specific CTL clones. (a) HLA-B*3501 molecules function as restriction elements for CTL clone C6. (b) HLA-Cw*0303 and -Cw*0304 molecules function as restriction elements for CTL clone B5. Autologous and allogeneic LCLs were used to stimulate clones B5 or C6 to produce IFN-γ spots. Single allele-matched LCLs were included and cultured with the CTLs (5×10^3) for 20 h. Each bar represents the mean number of spots in duplicate wells.

VYGGSKTSL, was not recognized, even at much higher concentrations.

Tetramers bind to the EBNA1-specific clone B5

As the peptide-dilution assay provided two optimal epitope candidates, we made fluorescently labelled tetramers incorporating the 10mer peptide FVYGGSKTSL or the 11mer VFVYGGSKTSL for further experiments. As shown in Fig. 5(d), these tetramers bound specifically to CTL clone B5. However, the tetramer incorporating the 10mer demonstrated higher avidity for the B5 clone than that incorporating the 11mer, suggesting the 10mer peptide FVYGGSKTSL to be the minimal and optimal epitope for the CTL. Moreover, clone B5 bound strongly to the HLA-Cw*0304 tetramer incorporating the 10mer, showing concordance with the results shown in Fig. 3(b). In addition, we characterized *in vitro*-expanded T cells from two donors by co-staining with MHC–peptide tetramer and CD62L. A proportion of 9.8% of HLA-Cw*0303-FVYGGSKTSL tetramer-positive lymphocytes were CD62-positive in one donor, and 6.5% in the other.

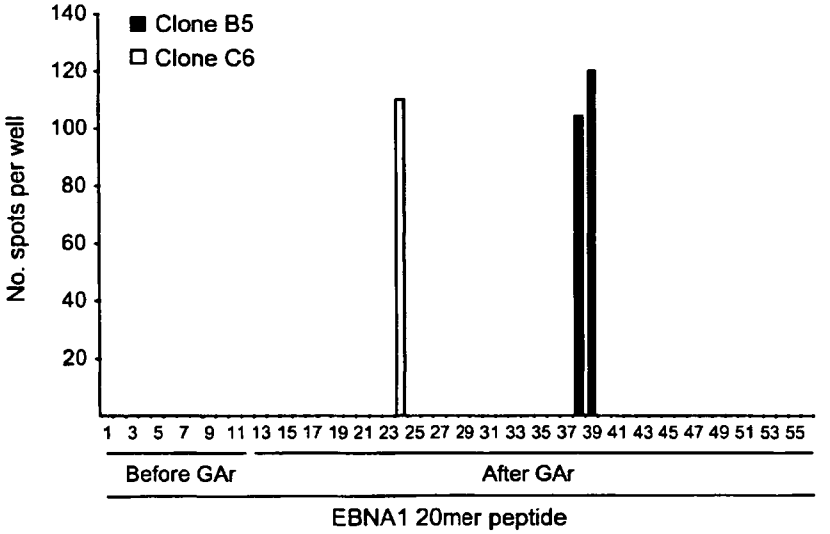

Fig. 4. Identification of overlapping peptides recognized by EBNA1-specific CTL clones. Autologous CD40-B cells (1×10^5 per well) were pulsed with 10 μg ml^{-1} of each of a set of 20mer overlapping peptides encompassing the EBNA1 protein, excluding GAr, and co-cultured with 5×10^2 CTL clone B5 or C6. Production of IFN-γ spots was then measured by ELISPOT assay.

Frequencies of EBNA1 epitope-specific $CD8^+$ T cells in PBMCs of healthy EBV-seropositive donors

We estimated frequencies of EBNA1 epitope-specific $CD8^+$ T cells in healthy EBV-seropositive donors by the mixed lymphocyte–peptide culture method. PBMCs from two donors with HLA-B*3501, one donor with HLA-Cw*0303 and three donors with HLA-Cw*0304 were tested. We could compare the anti-EBNA1 CTLp frequency in two donors with both HLA-B*3501 and HLA-Cw*0303 (HLA-Cw*0304). Representative tetramer staining of negative and positive microcultures from mixed lymphocyte–peptide culture wells is shown in Fig. 6. EBNA1-specific CTLp frequencies of HLA-B*3501-positive donors were 7.2×10^{-6} and 1.8×10^{-4}, and for HLA-Cw*0303 and -Cw*0304 were from 2.5×10^{-5} to $>2.1 \times 10^{-4}$. We did not find any hierarchy between the two EBNA1 epitopes in either of the donors with both HLA-B*3501 and HLA-Cw*0303 (Cw*0304) molecules (Table 1).

Effect of EBNA1-specific CTLs on EBV-infected B-cell growth

Clones B5 and C6 did not lyse autologous LCLs in the chromium-release assay (data not shown). Here, a final set of experiments was performed to ask whether these EBNA1-specific CTLs could affect the long-term growth and survival of EBNA1-expressing LCLs. Autologous and allogeneic LCLs with or without the restricting HLA molecules were seeded in 96-well plates in the presence or absence of responding CTLs. Cultures were then assayed for LCL outgrowth after 4 weeks. At the end, LCL outgrowth was assessed by microscopic inspection and confirmed by CD19 expression by flow cytometry. As shown in Fig. 7(a), both CTL clones clearly inhibited outgrowth of not only autologous LCLs, but also allogeneic LCLs with restricting HLA, suggesting that these CTL clones have the ability to inhibit outgrowth of EBV-positive cells with latency type III.

Recognition by EBNA1-specific CTL clone B5 of HLA-Cw*0303-transduced gastric carcinoma cells expressing EBNA1

Because naturally EBV-positive gastric cell lines are difficult to establish, we generated EBNA1-expressing gastric carcinoma cells designated MKN45-Cw0303-ΔGA-EBNA1 and MKN45-Cw0303-full-EBNA1 to verify that EBV-positive gastric cancer cell lines present the FVYGGSKTSL epitope. To investigate recognition by clone B5, we applied flow cytometry to detect EBNA1-specific CTLs producing IFN-γ. As shown in Fig. 7(b), 2.55% of B5 clone cells produced IFN-γ when co-cultured with MKN45-Cw0303-ΔGA-EBNA1 cells, demonstrating specific recognition of the FVYGGSKTSL epitope on cells transduced with GAr-deleted EBNA1. Otherwise, B5 clone cells did not produce IFN-γ when co-cultured with MKN45-Cw0303-full-EBNA1 cells.

DISCUSSION

Recently, EBNA1-specific CTLs were shown to recognize and lyse HLA-matched LCLs (Lee *et al.*, 2004; Tellam *et al.*, 2004; Voo *et al.*, 2004). In previous studies, such CTLs were generated from PBMCs of healthy donors after *in vitro* stimulation with autologous LCLs or EBNA1 peptide-pulsed PBMCs. As EBNA1 is expressed in all EBV-associated tumours and might be an important target for immunotherapy, we have explored the efficient induction of EBNA1-specific CTLs. Of the different methods used to obtain HLA class I-restricted epitopes on APCs for stimulation, we chose to employ full-length EBNA1 mRNA-transfected DCs. This strategy offers the following advantages: (i) the method is not dependent on knowledge of the HLA haplotype of each donor; (ii) there is complete deletion of antigenicity of the vector-backbone sequence; and (iii) the yield of mRNA *in vitro* transcription is highly reproducible and transduction is very efficient (Van

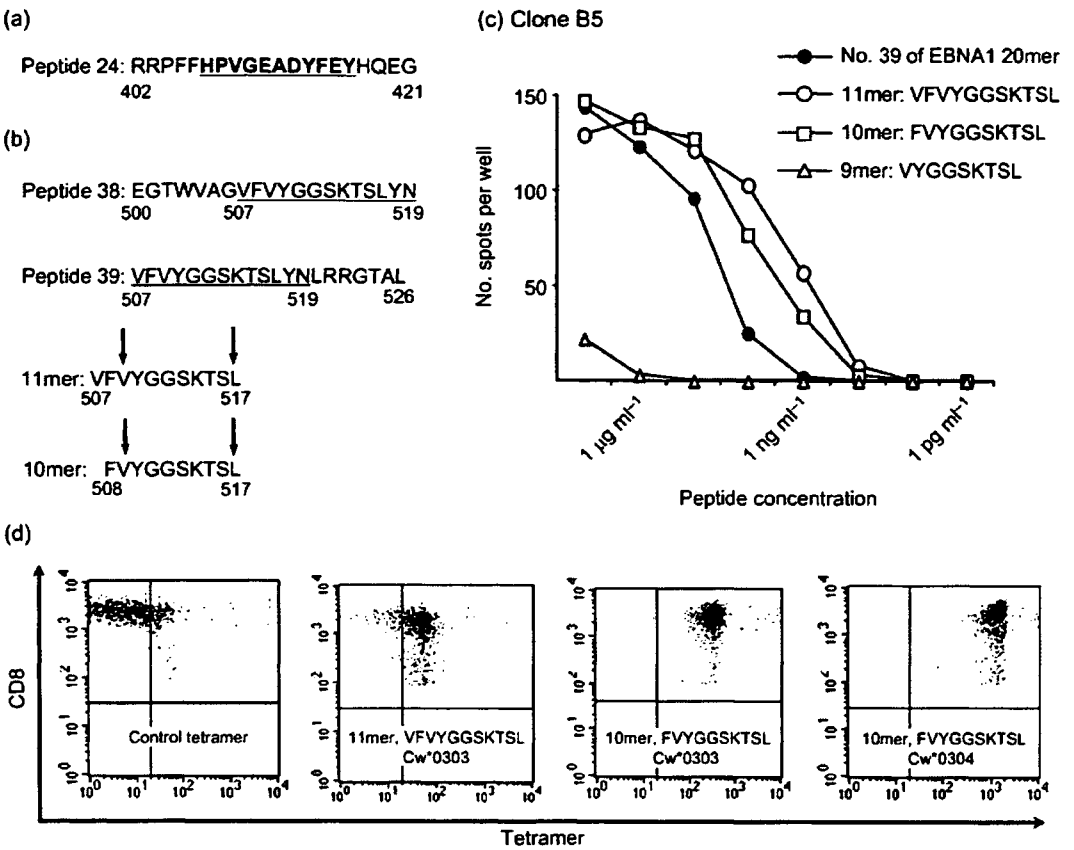

Fig. 5. Identification of optimal EBNA1 antigenic peptides recognized by EBNA1-specific CTL clones. (a) Amino acid sequence of the overlapping peptide recognized by the HLA-B*3501-restricted clone C6. The known epitope HPVGEADYFEY is indicated in bold and underlined. The numbers of the amino acid position in EBNA1 are shown. (b) Amino acid sequences of two consecutive overlapping peptides recognized by clone B5 and the potential optimal epitope sequences. The overlapping sequence between peptides 38 and 39 is underlined. Arrows indicate the primary and auxiliary anchors for HLA-Cw*0303 predicted by the program SYFPEITHI. The numbers of the amino acid positions in the EBNA1 protein are shown. (c) Titration of EBNA1-derived synthetic peptides. Autologous CD40-B cells were incubated for 1 h with 10-fold serial dilutions of synthetic peptides 507–526 (no. 39, 20mer), 507–517 (11mer), 508–17 (10mer) and 509–517 (9mer). CTL clone B5 (200 cells per well) was subsequently added and cultured for 20 h. Each symbol indicates the mean number of spots in duplicate wells. (d) The HLA-Cw*0303-restricted EBNA1-specific CTL clone B5 was stained with PE-conjugated HLA-Cw*0303–FVYGGSKTSL, HLA-Cw*0303–VFVYGGSKTSL or HLA-Cw*0304–FVYGGSKTSL tetrameric complexes and FITC-labelled anti-CD8 antibodies, and analysed by flow cytometry.

Tendeloo *et al.*, 2001). As an antigen, we used GAr-containing full-length EBNA1 instead of a GAr-deleted example to selectively activate CTL populations capable of reacting with epitopes that escape from the inhibitory mechanism governed by EBNA1 encoding GAr. Of note, even a low level of antigen delivery into DCs could induce antigen-specific CTL responses (Grunebach *et al.*, 2003), suggesting that this strategy has the potential to induce a CTL response even when a low density of EBNA1 epitopes is presented on DCs. In this study, we generated HLA-B- and -C-restricted EBNA1-specific CTLs successfully from a single donor, demonstrating that this method is a useful tool for generating EBNA1-specific CTLs, allowing investigation of the contribution of EBNA1 to cell-mediated immune responses in EBV-associated malignancies. Moreover, EBNA1 may have antigenicity when expressed on APCs, even if containing GAr *in vivo*. Finally, this induction method may be applicable for preparing EBNA1-specific CTLs for immunotherapy.

EBNA1 is generally immunologically invisible and only a small number of CTL epitopes have been identified (Blake *et al.*, 1997, 2000; Voo *et al.*, 2004). Of these, five epitopes are HLA-B-restricted and one is presented in the context of HLA-A. We detected two, one from HLA-B and another from HLA-C, from a single donor. To our knowledge, this is the first demonstration of an HLA-C-restricted EBNA1 epitope. To determine the minimal epitope, we compared

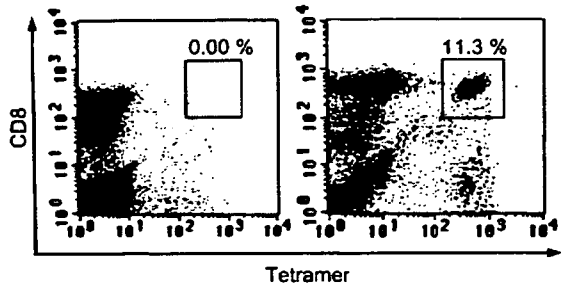

Fig. 6. Mixed lymphocyte–peptide culture analysis to estimate frequencies of C6 CTLp in $CD8^+$ lymphocytes of healthy EBV-seropositive donors. PBMCs from healthy EBV-seropositive donors with HLA-Cw*0303 were distributed at 2×10^5, 1×10^5 or 5×10^4 cells per well in 96-well round-bottomed plates in CTL medium with FVYGGSKTSL peptide (1 μg ml^{-1}) and IL-2 (20 U ml^{-1}). Half of the medium was replaced by fresh medium containing the relevant epitope peptide and IL-2 on day 7 and tetramer staining was performed on day 14. The plots show only data for $CD8^+$ lymphocytes, corresponding to 20–40 % of the cells in representative positive and negative cultures. The proportions of $CD8^+$ lymphocytes labelled specifically with the HLA-Cw*0303–FVYGGSKTSL tetramer are indicated.

the 11mer (VFVYGGSKTSL) and 10mer (FVYGGSKTSL) in a peptide-titration assay and found peptide concentration with half-maximal recognition of the target cells to be almost the same. However, clone C6 bound more strongly to tetramers incorporating the 10mer and we speculate that the N-terminal valine of the 11mer might be trimmed efficiently to yield 10mer in ELISPOT assay medium containing FCS. Moreover, the 10mer FVYGGSKTSL epitope was presented by HLA-Cw*0303 and -Cw*0304 molecules. As these two HLA-C alleles are possessed by > 35 % of Japanese, > 20 % of Northern Han Chinese (Hong *et al.*, 2005) and > 25 % of Caucasians, this new epitope should enable us to analyse cellular immunity to EBNA1 in a broad population. Indeed, we estimated $CD8^+$ T-cell frequencies specific to either FVYGGSKTSL or HPVGEADYFEY in PBMCs of healthy EBV-seropositive donors by the mixed lymphocyte–peptide culture method followed by tetramer staining and found that EBNA1-specific CTLp frequencies of HLA-B*3501- or HLA-Cw*0303 (and -Cw*0304)-positive donors were between 1×10^{-5} and 1×10^{-4}. These data provide useful information for understanding cellular immunity to EBNA1. For determination of frequencies of EBNA1 epitope-specific CTLs, the *ex vivo* ELISPOT assay (Blake *et al.*, 2000) is simple and readily applicable, because frequencies can be predicted at the level of 1×10^{-4} $CD8^+$ lymphocytes.

Adoptive immunotherapy with CTLs has proved feasible for preventing and treating EBV-associated PTLD, HD and NPC (Bollard *et al.*, 2004; Gottschalk *et al.*, 2005; Straathof *et al.*, 2005). With respect to the targets for EBV-specific CTLs, EBNA3s and LMP2 are major EBV latent antigens; EBNA3s are immunodominant and LMP2 is recognized frequently, but is subdominant. In contrast, CTL responses to other antigens (EBNA2, EBNA-LP, LMP1 and EBNA1) seem to be less frequent (Rickinson & Moss, 1997), although EBNA1 can be immunodominant in some EBV-seropositive donors (Blake *et al.*, 2000). Indeed, LCL-activated EBV-specific CTL lines from NPC patients for adoptive immunotherapy demonstrate stronger responses to the immunodominant EBNA3s than against LMP1 and LMP2 (Straathof *et al.*, 2005). In addition, tetramer and functional

Table 1. Frequencies of anti-EBNA1 CTL precursors

Donor	HLA-B*3501				HLA-Cw*0303/0304			
	$CD8^+$ (%)	PBMCs per well	Positive/tested wells	Frequency (among $CD8^+$)	$CD8^+$ (%)	PBMCs per well	Positive/tested wells	Frequency (among $CD8^+$)
Y01*	38	2×10^5	32/32	$> 1.8 \times 10^{-4}$	32	1×10^5	20/32	3.5×10^{-5}
		1×10^5	32/32			5×10^4	15/32	
		5×10^4	32/32			2.5×10^4	13/32	
T02†	32	2×10^5	10/32	7.2×10^{-6}	32	2×10^5	32/32	$> 2.1 \times 10^{-4}$
		1×10^5	7/32			1×10^5	32/32	
		5×10^4	5/32			5×10^4	32/32	
A03†		NA‡			23	2×10^5	20/32	2.5×10^{-5}
						1×10^5	13/32	
						5×10^4	12/32	
K04†		NA			19	2×10^5	18/32	2.7×10^{-5}
						1×10^5	13/32	
						5×10^4	11/32	

*HLA-Cw*0303.
†HLA-Cw*0304.
‡NA, Not available.

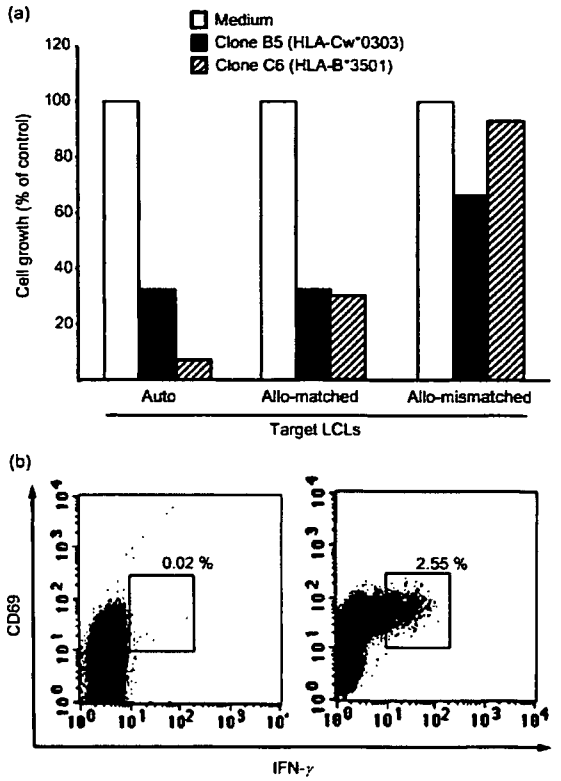

Fig. 7. Effects of EBNA1-specific CTLs on EBNA1-expressing cells. (a) EBNA1-specific CTL clones inhibit *in vitro* outgrowth of HLA-matched LCLs. Target LCLs (2×10^4) were cultured in triplicate wells of round-bottomed 96-well plates with EBNA1-specific CTL clones (1×10^4) or medium alone (control). After 4 weeks culture, the number of LCLs in the culture at each setting was counted. Cell growth (percentage of control) was calculated as [no. LCLs from the culture with CTLs (clone B5 or clone C6)]/[no. LCLs from the culture without CTLs (medium)] × 100. The B-cell (LCL) identity of the outgrowing cultures was confirmed by analysis of CD19 expression by flow cytometry. Data from one representative experiment of two are shown. (b) Detection of IFN-γ-producing anti-EBNA1 CTLs recognizing HLA-Cw*0303-positive cancer cells expressing EBNA1. B5 clones (5×10^5) were incubated with 2×10^6 MKN45-Cw0303 cells or MKN45-Cw0303-ΔGA-EBNA1 cells for 6 h, in the presence of brefeldin A for the last 5 h. After incubation, the cell suspensions were fixed with 4% paraformaldehyde in PBS and then permeabilized with IC Perm and stained with PE–cyanin-5.1-labelled anti-CD8, PE-labelled anti-CD69 or FITC-labelled anti-human IFN-γ mAbs. Stained cells were analysed by flow cytometry. Fifty thousand events were acquired for each analysis. The proportions of IFN-γ^+ CD69$^+$ CTLs among CD8$^+$ lymphocytes are indicated for one representative experiment of two performed.

analyses have shown that LMP2-specific CTLs are present in the infused CTLs used for adoptive immunotherapy and might have antiviral activity in patients with a good response to immunotherapy for HD (Bollard *et al.*, 2004). Interestingly, the CTL line from one NPC patient who attained a complete response was shown to contain a relatively large T-cell population for an EBNA1-derived CTL epitope (Straathof *et al.*, 2005). This suggests that increased attention should be focused on the contribution of EBNA1-specific CTLs to EBV cellular immunity. In this study, we showed two EBNA1-specific CTL clones to cause strong, specific inhibition of LCL outgrowth *in vitro*, which is consistent with recent observations with HLA-B8- and HLA-B*3501-restricted CTL clones (Tellam *et al.*, 2004; Voo *et al.*, 2004). C6 CTLs failed to respond to an HLA-Cw*0303-expressing gastric cancer cell line transduced with full-length EBNA1, although they produced IFN-γ when GAr-depleted EBNA1 was transduced (Fig. 7b). These data suggest differential antigen-processing machinery and presentation on class I molecules between LCLs and gastric cancer cells.

In conclusion, we have established EBNA1-specific CTL clones from PBMCs of a healthy donor by using EBNA1 mRNA-transfected DCs, and identified a novel CTL epitope of EBNA1 presented by HLA-Cw*0303 and -Cw*0304 molecules. The induction method adapted may be useful for generating EBNA1-specific CTLs and for investigating cellular immunity against EBNA1. Finally, the induced EBNA1-specific CTLs recognized EBNA1-expressing gastric carcinoma cells in the context of HLA-Cw*0303 *in vitro*, suggesting that EBNA1 is an important antigen for the further development of CTL therapy for EBV-associated malignancies.

ACKNOWLEDGEMENTS

The authors thank Dr H. Miyoshi, RIKEN BioResource Center, Ibaraki, Japan, for providing the lentiviral vectors, F. Ando for technical expertise and H. Tamaki and Y. Matsudaira for secretarial assistance. This work was supported in part by Grants-in-Aid for Scientific Research (C) (no. 17590428 and no. 18591212) from the Japan Society for the Promotion of Science, a Grant-in-Aid for Scientific Research on Priority Areas (no. 17016090 and no. 18015053) from the Ministry of Education, Culture, Science, Sports and Technology, Japan, and Third Team Comprehensive Control Research for Cancer (no. 30) from the Ministry of Health, Labour and Welfare, Japan.

REFERENCES

Akatsuka, Y., Goldberg, T. A., Kondo, E., Martin, E. G., Obata, Y., Morishima, Y., Takahashi, T. & Hansen, J. A. (2002). Efficient cloning and expression of HLA class I cDNA in human B-lymphoblastoid cell lines. *Tissue Antigens* **59**, 502–511.

Babcock, G. J., Hochberg, D. & Thorley-Lawson, A. D. (2000). The expression pattern of Epstein-Barr virus latent genes in vivo is dependent upon the differentiation stage of the infected B cell. *Immunity* **13**, 497–506.

Bai, Y., Soda, Y., Izawa, K., Tanabe, T., Kang, X., Tojo, A., Hoshino, H., Miyoshi, H., Asano, S. & Tani, K. (2003). Effective transduction and stable transgene expression in human blood cells by a third-generation lentiviral vector. *Gene Ther* **10**, 1446–1457.

Bickham, K., Munz, C., Tsang, M. L., Larsson, M., Fonteneau, J. F., Bhardwaj, N. & Steinman, R. (2001). EBNA1-specific CD4+ T cells

in healthy carriers of Epstein-Barr virus are primarily Th1 in function. *J Clin Invest* **107**, 121–130.

Blake, N., Lee, S., Redchenko, I., Thomas, W., Steven, N., Leese, A., Steigerwald-Mullen, P., Kurilla, M. G., Frappier, L. & Rickinson, A. (1997). Human CD8+ T cell responses to EBV EBNA1: HLA class I presentation of the (Gly-Ala)-containing protein requires exogenous processing. *Immunity* **7**, 791–802.

Blake, N., Haigh, T., Shaka'a, G., Croom-Carter, D. & Rickinson, A. (2000). The importance of exogenous antigen in priming the human CD8+ T cell response: lessons from the EBV nuclear antigen EBNA1. *J Immunol* **165**, 7078–7087.

Bollard, C. M., Aguilar, L., Straathof, K. C., Gahn, B., Huls, M. H., Rousseau, A., Sixbey, J., Gresik, M. V., Carrum, G. & other authors (2004). Cytotoxic T lymphocyte therapy for Epstein-Barr virus+ Hodgkin's disease. *J Exp Med* **200**, 1623–1633.

Callan, M. F., Tan, L., Annels, N., Ogg, G. S., Wilson, J. D., O'Callaghan, C. A., Steven, N., McMichael, A. J. & Rickinson, A. B. (1998). Direct visualization of antigen-specific CD8+ T cells during the primary immune response to Epstein-Barr virus in vivo. *J Exp Med* **187**, 1395–1402.

Coulie, P. G., Karanikas, V., Colau, D., Lurquin, C., Landry, C., Marchand, M., Dorval, T., Brichard, V. & Boon, T. (2001). A monoclonal cytolytic T-lymphocyte response observed in a melanoma patient vaccinated with a tumor-specific antigenic peptide encoded by gene MAGE-3. *Proc Natl Acad Sci U S A* **98**, 10290–10295.

Dauer, M., Obermaier, B., Herten, J., Haerle, C., Pohl, K., Rothenfusser, S., Schnurr, M., Endres, S. & Eigler, A. (2003). Mature dendritic cells derived from human monocytes within 48 hours: a novel strategy for dendritic cell differentiation from blood precursors. *J Immunol* **170**, 4069–4076.

Gottschalk, S., Rooney, C. M. & Heslop, H. E. (2005). Post-transplant lymphoproliferative disorders. *Annu Rev Med* **56**, 29–44.

Grunebach, F., Muller, M. R., Nencioni, A. & Brossart, P. (2003). Delivery of tumor-derived RNA for the induction of cytotoxic T-lymphocytes. *Gene Ther* **10**, 367–374.

Heiser, A., Dahm, P., Yancey, D. R., Maurice, M. A., Boczkowski, D., Nair, S. K., Gilboa, E. & Vieweg, J. (2000). Human dendritic cells transfected with RNA encoding prostate-specific antigen stimulate prostate-specific CTL responses in vitro. *J Immunol* **164**, 5508–5514.

Heiser, A., Coleman, D., Dannull, J., Yancey, D., Maurice, M. A., Lallas, C. D., Dahm, P., Niedzwiecki, D., Gilboa, E. & Vieweg, J. (2002). Autologous dendritic cells transfected with prostate-specific antigen RNA stimulate CTL responses against metastatic prostate tumors. *J Clin Invest* **109**, 409–417.

Hong, W., Fu, Y., Chen, S., Wang, F., Ren, X. & Xu, A. (2005). Distributions of HLA class I alleles and haplotypes in Northern Han Chinese. *Tissue Antigens* **66**, 297–304.

Khanna, R., Burrows, S. R., Kurilla, M. G., Jacob, C. A., Misko, I. S., Sculley, T. B., Kieff, E. & Moss, D. J. (1992). Localization of Epstein-Barr virus cytotoxic T cell epitopes using recombinant vaccinia: implications for vaccine development. *J Exp Med* **176**, 169–176.

Khanna, R., Burrows, S. R., Steigerwald-Mullen, P. M., Thomson, S. A., Kurilla, M. G. & Moss, D. J. (1995). Isolation of cytotoxic T lymphocytes from healthy seropositive individuals specific for peptide epitopes from Epstein-Barr virus nuclear antigen 1: implications for viral persistence and tumor surveillance. *Virology* **214**, 633–637.

Khanna, R., Burrows, S. R., Steigerwald-Mullen, P. M., Moss, D. J., Kurilla, M. G. & Cooper, L. (1997). Targeting Epstein-Barr virus nuclear antigen 1 (EBNA1) through the class II pathway restores immune recognition by EBNA1-specific cytotoxic T lymphocytes: evidence for HLA-DM-independent processing. *Int Immunol* **9**, 1537–1543.

Kieff, E. & Rickinson, A. B. (2001). Epstein-Barr virus and its replication. In *Fields Virology*, 4th edn, pp. 2511–2573. Edited by D. M. Knipe & P. M. Howley. Philadelphia, PA: Lippincott Williams & Wilkins.

Kondo, E., Topp, M. S., Kiem, H. P., Obata, Y., Morishima, Y., Kuzushima, K., Tanimoto, M., Harada, M., Takahashi, T. & Akatsuka, Y. (2002). Efficient generation of antigen-specific cytotoxic T cells using retrovirally transduced CD40-activated B cells. *J Immunol* **169**, 2164–2171.

Kruger, S., Schroers, R., Rooney, C. M., Gahn, B. & Chen, S. Y. (2003). Identification of a naturally processed HLA-DR-restricted T-helper epitope in Epstein-Barr virus nuclear antigen type 1. *J Immunother* **26**, 212–221.

Kuzushima, K., Hoshino, Y., Fujii, K., Yokoyama, N., Fujita, M., Kiyono, T., Kimura, H., Morishima, T., Morishima, Y. & Tsurumi, T. (1999). Rapid determination of Epstein-Barr virus-specific CD8(+) T-cell frequencies by flow cytometry. *Blood* **94**, 3094–3100.

Kuzushima, K., Hayashi, N., Kimura, H. & Tsurumi, T. (2001). Efficient identification of HLA-A*2402-restricted cytomegalovirus-specific CD8(+) T-cell epitopes by a computer algorithm and an enzyme-linked immunospot assay. *Blood* **98**, 1872–1881.

Kuzushima, K., Hayashi, N., Kudoh, A., Akatsuka, Y., Tsujimura, K., Morishima, Y. & Tsurumi, T. (2003). Tetramer-assisted identification and characterization of epitopes recognized by HLA A*2402-restricted Epstein-Barr virus-specific CD8+ T cells. *Blood* **101**, 1460–1468.

Lee, S. P., Brooks, J. M., Al-Jarrah, H., Thomas, W. A., Haigh, T. A., Taylor, G. S., Humme, S., Schepers, A., Hammerschmidt, W. & other authors (2004). CD8 T cell recognition of endogenously expressed Epstein-Barr virus nuclear antigen 1. *J Exp Med* **199**, 1409–1420.

Leen, A., Meij, P., Redchenko, I., Middeldorp, J., Bloemena, E., Rickinson, A. & Blake, N. (2001). Differential immunogenicity of Epstein-Barr virus latent-cycle proteins for human CD4(+) T-helper 1 responses. *J Virol* **75**, 8649–8659.

Levitskaya, J., Coram, M., Levitsky, V., Imreh, S., Steigerwald-Mullen, P. M., Klein, G., Kurilla, M. G. & Masucci, M. G. (1995). Inhibition of antigen processing by the internal repeat region of the Epstein-Barr virus nuclear antigen-1. *Nature* **375**, 685–688.

Levitskaya, J., Sharipo, A., Leonchiks, A., Ciechanover, A. & Masucci, M. G. (1997). Inhibition of ubiquitin/proteasome-dependent protein degradation by the Gly-Ala repeat domain of the Epstein-Barr virus nuclear antigen 1. *Proc Natl Acad Sci U S A* **94**, 12616–12621.

Muller, M. R., Tsakou, G., Grunebach, F., Schmidt, S. M. & Brossart, P. (2004). Induction of chronic lymphocytic leukemia (CLL)-specific CD4- and CD8-mediated T-cell responses using RNA-transfected dendritic cells. *Blood* **103**, 1763–1769.

Munz, C., Bickham, K. L., Subklewe, M., Tsang, M. L., Chahroudi, A., Kurilla, M. G., Zhang, D., O'Donnell, M. & Steinman, R. M. (2000). Human CD4(+) T lymphocytes consistently respond to the latent Epstein-Barr virus nuclear antigen EBNA1. *J Exp Med* **191**, 1649–1660.

Murray, R. J., Kurilla, M. G., Brooks, J. M., Thomas, W. A., Rowe, M., Kieff, E. & Rickinson, A. B. (1992). Identification of target antigens for the human cytotoxic T cell response to Epstein-Barr virus (EBV): implications for the immune control of EBV-positive malignancies. *J Exp Med* **176**, 157–168.

Nair, S. K., Boczkowski, D., Morse, M., Cumming, R. I., Lyerly, H. K. & Gilboa, E. (1998). Induction of primary carcinoembryonic antigen (CEA)-specific cytotoxic T lymphocytes in vitro using human dendritic cells transfected with RNA. *Nat Biotechnol* **16**, 364–369.

Nair, S. K., Heiser, A., Boczkowski, D., Majumdar, A., Naoe, M., Lebkowski, J. S., Vieweg, J. & Gilboa, E. (2000). Induction of cytotoxic T cell responses and tumor immunity against unrelated

tumors using telomerase reverse transcriptase RNA transfected dendritic cells. *Nat Med* 6, 1011–1017.

Paludan, C., Bickham, K., Nikiforow, S., Tsang, M. L., Goodman, K., Hanekom, W. A., Fonteneau, J. F., Stevanovic, S. & Munz, C. (2002). Epstein-Barr nuclear antigen 1-specific CD4(+) Th1 cells kill Burkitt's lymphoma cells. *J Immunol* **169**, 1593–1603.

Rammensee, H., Bachmann, J., Emmerich, N. P., Bachor, O. A. & Stevanovic, S. (1999). SYFPEITHI: database for MHC ligands and peptide motifs. *Immunogenetics* **50**, 213–219.

Rickinson, A. B. & Moss, D. J. (1997). Human cytotoxic T lymphocyte responses to Epstein-Barr virus infection. *Annu Rev Immunol* 15, 405–431.

Rickinson, A. B. & Kieff, E. (2001). Epstein-Barr Virus. In *Fields Virology*, 4th edn, pp. 2575–2627. Edited by D. M. Knipe & P. M. Howley. Philadelphia, PA: Lippincott Williams & Wilkins.

Romani, N., Gruner, S., Brang, D., Kampgen, E., Lenz, A., Trockenbacher, B., Konwalinka, G., Fritsch, P. O., Steinman, R. M. & Schuler, G. (1994). Proliferating dendritic cell progenitors in human blood. *J Exp Med* **180**, 83–93.

Sallusto, F. & Lanzavecchia, A. (1994). Efficient presentation of soluble antigen by cultured human dendritic cells is maintained by granulocyte/macrophage colony-stimulating factor plus interleukin 4 and downregulated by tumor necrosis factor alpha. *J Exp Med* **179**, 1109–1118.

Schultze, J. L., Michalak, S., Seamon, M. J., Dranoff, G., Jung, K., Daley, J., Delgado, J. C., Gribben, J. G. & Nadler, L. M. (1997). CD40-activated human B cells: an alternative source of highly efficient antigen presenting cells to generate autologous antigen-specific T cells for adoptive immunotherapy. *J Clin Invest* **100**, 2757–2765.

Steven, N. M., Leese, A. M., Annels, N. E., Lee, S. P. & Rickinson, A. B. (1996). Epitope focusing in the primary cytotoxic T cell response to Epstein-Barr virus and its relationship to T cell memory. *J Exp Med* **184**, 1801–1813.

Straathof, K. C., Bollard, C. M., Popat, U., Huls, M. H., Lopez, T., Morriss, M. C., Gresik, M. V., Gee, A. P., Russell, H. V. & other authors (2005). Treatment of nasopharyngeal carcinoma with Epstein-Barr virus-specific T lymphocytes. *Blood* **105**, 1898–1904.

Su, Z., Dannull, J., Heiser, A., Yancey, D., Pruitt, S., Madden, J., Coleman, D., Niedzwiecki, D., Gilboa, E. & Vieweg, J. (2003). Immunological and clinical responses in metastatic renal cancer patients vaccinated with tumor RNA-transfected dendritic cells. *Cancer Res* **63**, 2127–2133.

Tellam, J., Connolly, G., Green, K. J., Miles, J. J., Moss, D. J., Burrows, S. R. & Khanna, R. (2004). Endogenous presentation of CD8+ T cell epitopes from Epstein-Barr virus-encoded nuclear antigen 1. *J Exp Med* **199**, 1421–1431.

Van Tendeloo, V. F., Ponsaerts, P., Lardon, F., Nijs, G., Lenjou, M., Van Broeckhoven, C., Van Bockstaele, D. R. & Berneman, Z. N. (2001). Highly efficient gene delivery by mRNA electroporation in human hematopoietic cells: superiority to lipofection and passive pulsing of mRNA and to electroporation of plasmid cDNA for tumor antigen loading of dendritic cells. *Blood* **98**, 49–56.

Voo, K. S., Fu, T., Heslop, H. E., Brenner, M. K., Rooney, C. M. & Wang, R. F. (2002). Identification of HLA-DP3-restricted peptides from EBNA1 recognized by CD4(+) T cells. *Cancer Res* **62**, 7195–7199.

Voo, K. S., Fu, T., Wang, H. Y., Tellam, J., Heslop, H. E., Brenner, M. K., Rooney, C. M. & Wang, R. F. (2004). Evidence for the presentation of major histocompatibility complex class I-restricted Epstein-Barr virus nuclear antigen 1 peptides to CD8+ T lymphocytes. *J Exp Med* **199**, 459–470.

Yin, Y., Manoury, B. & Fahraeus, R. (2003). Self-inhibition of synthesis and antigen presentation by Epstein-Barr virus-encoded EBNA1. *Science* **301**, 1371–1374.

Zeis, M., Siegel, S., Wagner, A., Schmitz, M., Marget, M., Kuhl-Burmeister, R., Adamzik, I., Kabelitz, D., Dreger, P. & other authors (2003). Generation of cytotoxic responses in mice and human individuals against hematological malignancies using survivin-RNA-transfected dendritic cells. *J Immunol* **170**, 5391–5397.

From www.bloodjournal.org at AICHI CNCR CTR on March 24, 2008. For personal use only.

Plenary paper

High-risk HLA allele mismatch combinations responsible for severe acute graft-versus-host disease and implication for its molecular mechanism

Takakazu Kawase,[1] Yasuo Morishima,[2] Keitaro Matsuo,[3] Koichi Kashiwase,[4] Hidetoshi Inoko,[5] Hiroh Saji,[6] Shunichi Kato,[7] Takeo Juji,[8] Yoshihisa Kodera,[9] and Takehiko Sasazuki,[10] for The Japan Marrow Donor Program

[1]Division of Immunology, Aichi Cancer Center, Nagoya; [2]Department of Hematology and Cell Therapy, Aichi Cancer Center, Nagoya; [3]Division of Epidemiology and Prevention, Aichi Cancer Center, Nagoya; [4]Japanese Red Cross Tokyo Metropolitan Blood Center, Tokyo; [5]Division of Molecular Science, Tokai University School of Medicine, Isehara; [6]Human Leukocyte Antigen (HLA) Laboratory, Nonprofit Organization (NPO), Kyoto; [7]Department of Cell Transplantation and Regenerative Medicine, Tokai University School of Medicine, Isehara; [8]Japanese Red Cross Central Blood Institute, Tokyo; [9]Japanese Red Cross Nagoya First Hospital, Nagoya; [10]International Medical Center of Japan, Tokyo, Japan

In allogenic hematopoietic stem-cell transplantation, an effect of HLA locus mismatch in allele level on clinical outcome has been clarified. However, the effect of each HLA allele mismatch combination is little known, and its molecular mechanism to induce acute graft-versus-host disease (aGVHD) remains to be elucidated. A total of 5210 donor-patient pairs who underwent transplantation through Japan Marrow Donor Program were analyzed. All HLA-A, -B, -C, -DRB1, -DQB1, and -DPB1 alleles were retrospectively typed in all pairs. The impacts of the HLA allele mismatch combinations and amino acid substitution positions in 6 HLA loci on severe aGVHD were analyzed. A total of 15 significant high-risk HLA allele mismatch combinations and 1 HLA-DRB1-DQB1 linked mismatch combinations (high-risk mismatch) for severe aGVHD were identified, and the number of high-risk mismatches was highly associated with the occurrence of severe aGVHD regardless of the presence of mismatch combinations other than high-risk mismatch. Furthermore, 6 specific amino acid substitution positions in HLA class I were identified as those responsible for severe aGVHD. These findings provide evidence to elucidate the mechanism of aGVHD on the basis of HLA molecule. Furthermore, the identification of high-risk mismatch, that is, nonpermissive mismatch, would be beneficial for the selection of a suitable donor. (Blood. 2007;110:2235-2241)

© 2007 by The American Society of Hematology

Introduction

Allogenic hematopoietic stem-cell transplantation (HSCT) from an HLA-matched unrelated (UR) donor has been established as a treatment for hematologic malignancies, when an HLA-identical sibling donor is unavailable.[1,2] When a matched unrelated donor was not found in the donor registry, a partially HLA-matched unrelated donor was one of the candidates for alternative donor. But the higher risk of immunologic events, especially graft-versus-host disease (GVHD), was an important drawback. Extensive recent research has accumulated evidence of the role of each HLA locus mismatch on clinical outcome for UR-HSCT,[3-9] which has made it easy to search and select a partially matched donor. To further expand options for donor selection, our next challenge is to identify permissive and nonpermissive mismatch combinations of each HLA allele. Although there were some divisional trials with small populations,[10,11] a large-scale cohort is essential for comprehensive analysis to identify nonpermissive mismatch combinations that are significant risk factors for severe acute graft-versus-host disease (aGVHD).

In this study, we identified nonpermissive HLA mismatch allele combinations of all major 6 HLA loci, and their responsible positions of amino acid substitution for aGVHD.

Patients, materials, and methods

Patients

A total of 5210 donor-patient pairs who underwent transplantation through the Japan Marrow Donor Program (JMDP) with T-cell–replete marrow from a serologically HLA-A, -B, and -DR antigen-matched donor between January 1993 and January 2006 were analyzed in this cohort study. Patients who received a transplant of harvested marrow outside Japan (n = 51) or were unavailable for blood sample (n = 428) were not eligible for this study of a total of 5689 consecutively registered patients.

Patient characteristics are shown in Table S1, available on the *Blood* website (see the Supplemental Materials link at the top of the online article). The final clinical survey of these patients was completed by June 1, 2006. Informed consent was obtained from patients and donors in accordance with the Declaration of Helsinki, and approval of the study was obtained from the Institutional Review Board of Aichi Cancer Center and JMDP.

HLA typing of patients and donors

Alleles at the HLA-A, -B, -C, -DRB1, -DQB1, and -DPB1 loci were identified by the methods described previously.[4,5] Six HLA locus alleles were typed in all 5210 pairs. HLA genotypes of HLA-A, -B, -C, -DQB1, and -DPB1 allele of patient and donor were reconfirmed by the Luminex microbead method (Luminex 100 System; Luminex, Austin, TX). For convenience, we showed the frequency of HLA alleles that existed with

Submitted February 6, 2007; accepted June 4, 2007. Prepublished online as *Blood* First Edition paper, June 6, 2007; DOI 10.1182/blood-2007-02-072405.

The online version of this article contains a data supplement.

The publication costs of this article were defrayed in part by page charge payment. Therefore, and solely to indicate this fact, this article is hereby marked "advertisement" in accordance with 18 USC section 1734.

© 2007 by The American Society of Hematology

From www.bloodjournal.org at AICHI CNCR CTR on March 24, 2008. For personal use only.

more than a 5% allele frequency in the current Japanese data set and less than a 1% allele frequency in white populations[12] in Table S2.

Matching of HLA allele between patient and donor

For the analysis of aGVHD, HLA allele mismatch among the donor-recipient pair was scored when the recipient's alleles were not shared by the donor (GVH vector). We also used GVH vectors for the analysis of overall survival (OS) to indicate OS of aGVHD high-risk or low-risk group.

Evaluation of acute GVHD

Occurrences of aGVHD were graded with grade 0, I, II, III, and IV according to established criteria.[13] Grades III and IV were defined as severe aGVHD.

Definitions of amino acid substitution

Amino acid sequences of HLA-A, -B, -C, -DR, -DQ, and -DP molecules were obtained from IMGT/HLA sequence database.[14] For example, Tyr9A-Phe9A indicated amino acid substitutions of position 9 in HLA-A molecule at which the donor had tyrosine and the patient phenylalanine. Substituted amino acids in HLA class I were summarized in Tables S3-S5.

Definition of nonpermissive HLA combinations

We defined the nonpermissive HLA allele combination as a significant risk factor for severe aGVHD, because severe aGVHD was a solid marker for alloreactivity in HSCT and was the main contributor to transplantation-related mortality.[15,16]

Definition of hydropathy scale

The hydropathy scale proposed by Kyte and Doolittle[17] evaluates the hydrophilicity and hydrophobicity of 20 amino acids to estimate the protein structure. Hydrophobic amino acid has a plus value and hydrophilic amino acid a minus value, and their absolute value indicates the grade of each property.

Statistical analysis

Cumulative incidences of aGVHD were assessed by the method described elsewhere to eliminate the effect of competing risk.[18,19] The competing event regarding aGVHD was defined as death without aGVHD. A log-rank test was applied to assess the impact by the factor of interest. Multivariable Cox regression analyses[20] were conducted to evaluate the impact of HLA allele mismatch combination, and the positions and types of amino acid substitution (for example, alanine, arginine, asparagines) of HLA molecules.

The HLA mismatch combination was evaluated for each locus separately, and the HLA match and HLA one-locus mismatch in every locus were analyzed. For example, A0206-A0201 mismatch combination meant that the donor has HLA-A*0206, recipient has HLA-A*0201, and another HLA-A allele of each donor and recipient was identical. This mismatch was compared with the HLA-A allele match. The mismatch combination of which the number of pairs was less than 10 was lumped together as "other mismatch." This is because, according to the computer simulation by Peduzzi et al,[21] it is generally accepted that regression analysis for a variable having fewer than 10 events might give an unreliable estimation. The model was constructed with mismatch combinations, mismatch status in other loci (match, 1 locus mismatch, and 2 locus mismatches as ordinal variable), and potential confounders. Confounders considered were sex (donor-recipient pairs), patient age (linear), donor age (linear), type of disease, risk of leukemia relapse (standard, high, and diseases other than leukemia), GVHD prophylaxis (cyclosporine [CSP] vs FK 506 [FK]), ATG (ATG vs no ATG), and preconditioning (total body irradiation [TBI] vs non-TBI). We used these confounders in all analyses in this paper to keep results comparable.

The impact of positions and types of amino acid substitution in HLA molecules was evaluated in pairs with HLA one-locus mismatch in HLA-A, -B, -C, -DRB1, -DQB1, and -DPB1 separately. The amino acid positions we analyzed were all those at which amino acid was substituted in each locus. We analyzed the impact of each amino acid substitution on each position separately. Multivariable Cox models including positions and types of amino acid substitution, mismatch status in other loci (match, 1 locus mismatch, and 2 locus mismatches as ordinal variable), and confounders described in "Statistical analysis" were constructed.

We applied a P value of less than .005 as statistically significant to eliminate false-positive associations. All the analyses were conducted by STATA version 9.2 (Stata, College Station, TX).

Validation of statistical analysis

We validated the statistical analysis using 2 methods, traditional training-and-test method and bootstrap resampling method, in HLA-A analysis to confirm the usability of bootstrap resampling. In the traditional training-and-test method, donor-recipient pairs were divided at random in 2 equally scaled groups, group A and group B. When consistent results were obtained in both analyses, we considered the results as validated. In the bootstrap resampling method,[22] we estimated the measure of association with the resampled data repeatedly drawn from the original data. Although around 100 to 200 bootstrapped samplings are generally sufficient,[23] we explored 500, 1000, 5000, 10 000, and 50 000 bootstrappings in analysis of HLA-A mismatch combinations. We confirmed that an analysis using more than 5000 bootstrappings made the results stable. Because there was high concordance between these 2 methods (Table S6), we adopted bootstrap resampling using 10 000 bootstrap samples for all analyses in this paper as the method for validation. This is because traditional training-and-test methods do not work efficiently when small subgroups are considered as in this paper. Only when the results of base analysis and validating analysis using bootstrap resampling were significant concurrently were the results of the analysis judged to be statistically significant. When the result of base analysis was significant but the result of validating analysis using bootstrap resampling was not, we indicated this by adding an asterisk next to the P value of the base analysis.

Results

Impact of HLA allele mismatch combinations on severe aGVHD

Hazard ratios (HRs) of HLA allele mismatch combinations in HLA-A and -C on severe aGVHD are shown in Table 1 (HLA-B, -DR, -DQ, and -DP are available in Table S7).

In HLA-A locus mismatch combinations, A*0206-A*0201 (HR: 1.78; CI, 1.32-2.41), A*0206-A*0207 (HR: 3.45; CI: 2.09-5.70), A*2602-A*2601 (HR: 3.35; CI: 1.89-5.91), and A*2603-A*2601 (HR: 2.17; CI: 1.29-3.64), were significant risk factors for severe aGVHD.

In HLA-C locus mismatch combinations, 7 combinations were significant risk factors for severe aGVHD; those were as follows: Cw*0401-Cw*0303 (HR: 2.81; CI: 1.72-4.60), Cw*0801-Cw*0303 (HR: 2.32; CI: 1.58-3.40), Cw*0303-Cw*1502 (HR: 3.22; CI: 1.75-5.89), Cw*0304-Cw*0801 (HR: 2.34; CI: 1.55-3.52), Cw*1402-Cw*0304 (HR: 3.66; CI: 2.00-6.68), Cw*1502-Cw*0,304 (HR: 3.77; CI: 2.20-6.47), and Cw*1502-Cw*1402 (HR: 4.97; CI: 3.41-7.25). To summarize, high-risk HLA allele mismatch combinations for severe aGVHD, that is, nonpermissive mismatch combinations, of all major 6 HLA loci were listed in Table 2. A total of 15 nonpermissive HLA allele mismatch combinations (4 in HLA-A, 1 in HLA-B, 7 in HLA-C, 1 in HLA-DRB1, and 2 in HLA-DPB1) and 1 HLA-DRB1-DQB1 linked mismatch combination (Table 2 legend) were identified.

We divided donor-recipient pairs into 4 groups according to the number of nonpermissive mismatches: (1) full match (in HLA-A, -B, -C, -DRB1, -DQB1, and -DPB1) group; (2) zero nonpermissive mismatch (with mismatches other than nonpermissive mismatches)

From www.bloodjournal.org at AICHI CNCR CTR on March 24, 2008. For personal use only.

Table 1. Multivariable analysis of impact of mismatch pairs for sever aGVHD in HLA-A and -C

Mismatch combination, donor-patient	N	HR (95% CI)	P
A locus match	4510	1	NA
A0201-A0206	138	1.23 (0.87-1.73)	.223
A0206-A0201	131	1.78 (1.32-2.41)	< .001
A0201-A0207	28	0.83 (0.34-2.03)	.699
A0207-A0201	20	1.12 (0.42-3.02)	.809
A0201-A0210	11	1.57 (0.58-4.23)	.367
A0206-A0207	27	3.45 (2.09-5.70)	< .001
A0207-A0206	22	0.71 (0.23-2.24)	.571
A2402-A2420	60	0.64 (0.32-1.30)	.225
A2420-A2402	30	1.18 (0.56-2.49)	.66
A2601-A2602	24	0.64 (0.26-1.58)	.34
A2602-A2601	21	3.35 (1.89-5.91)	< .001
A2601-A2603	34	1.37 (0.73-2.57)	.326
A2603-A2601	35	2.17 (1.29-3.64)	.003
A2602-A2603	10	1.23 (0.30-4.98)	.763
A2603-A2602	12	1.50 (0.48-4.68)	.485
A other mismatch	97	1.47 (1.00-2.15)	.047
C locus match	3685	1	NA
C0102-C0303	30	2.83 (1.50-5.32)	.001*
C0303-C0102	38	1.05 (0.47-2.36)	.899
C0102-C0304	12	1.85 (0.59-5.81)	.287
C0304-C0102	19	0.89 (0.28-2.79)	.854
C0102-C0401	14	1.87 (0.77-4.55)	.164
C0102-C0803	24	1.97 (0.87-4.42)	.099
C0803-C0102	10	1.66 (0.53-5.19)	.383
C0102-C1402	16	3.86 (1.98-7.51)	< .001*
C1402-C0102	13	0.46 (0.06-3.33)	.45
C0303-C0304	83	1.08 (0.63-1.85)	.761
C0304-C0303	62	0.83 (0.41-1.68)	.614
C0303-C0401	31	1.73 (0.89-3.36)	.103
C0401-C0303	42	2.81 (1.72-4.60)	< .001
C0303-C0702	25	1.16 (0.52-2.62)	.706
C0702-C0303	18	2.16 (0.96-4.85)	.062
C0303-C0801	76	1.07 (0.63-1.84)	.782
C0801-C0303	80	2.32 (1.58-3.40)	< .001
C0303-C1502	25	3.22 (1.75-5.89)	< .001
C0304-C0401	15	3.02 (1.34-6.79)	.007
C0401-C0304	12	6.22 (3.07-12.5)	< .001*
C0304-C0702	26	2.35 (1.16-4.76)	.017
C0702-C0304	33	1.22 (0.58-2.59)	.59
C0304-C0801	69	2.34 (1.55-3.52)	< .001
C0801-C0304	47	1.64 (0.98-2.76)	.057
C0304-C1402	28	3.06 (1.68-5.60)	< .001*
C1402-C0304	23	3.66 (2.00-6.68)	< .001
C0304-C1502	53	1.82 (1.08-3.05)	.023
C1502-C0304	27	3.77 (2.20-6.47)	< .001
C0801-C0102	10	2.88 (0.92-9.03)	.068
C0801-C0803	27	1.55 (0.69-3.48)	.284
C0803-C0801	26	2.04 (1.04-3.99)	.037
C0801-C1502	36	1.59 (0.79-3.21)	.19
C1502-C0801	23	2.28 (1.07-4.85)	.031
C1402-C1502	55	1.67 (1.01-2.77)	.043
C1502-C1402	50	4.97 (3.41-7.25)	< .001
C other mismatch	347	1.69 (1.34-2.14)	< .001

A0206-A0201 mismatch combination meant that the donor has HLA-A*0206, recipient has HLA-A*0201 and another HLA-A allele of each donor and recipient was identical. Each mismatch pair in HLA-A was compared with the HLA-A allele match, and each mismatch pair in HLA-C was compared with the HLA-C allele match. Confounders considered were sex (donor-recipient pairs), patient age (linear), donor age (linear), type of disease, risk of leukemia relapse (standard, high and diseases other than leukemia), GVHD prophylaxis, (CSP vs. FK), ATG (ATG vs. no ATG) and preconditioning (TBI vs non-TBI).

HR denotes hazard ratio; CI, confidence interval; NA, not applicable.

*The result of base analysis was significant, but the result of validating analysis using bootstrap resampling was not. The results of the analysis were thus judged not to be statistically significant.

Table 2. Nonpermissive allele mismatch combinations for severe aGVHD

Mismatch combination, donor-patient	N	HR (95% CI)	P
A0206-A0201	131	1.78 (1.32-2.41)	< .001
A0206-A0207	27	3.45 (2.09-5.70)	< .001
A2602-A2601	21	3.35 (1.89-5.91)	< .001
A2603-A2601	35	2.17 (1.29-3.64)	.003
B1501-B1507	19	3.34 (1.85-5.99)	< .001
C0303-C1502	25	3.22 (1.75-5.89)	< .001
C0304-C0801	69	2.34 (1.55-3.52)	< .001
C0401-C0303	42	2.81 (1.72-4.60)	< .001
C0801-C0303	80	2.32 (1.58-3.40)	< .001
C1402-C0304	23	3.66 (2.00-6.68)	< .001
C1502-C0304	27	3.77 (2.20-6.47)	< .001
C1502-C1402	50	4.97 (3.41-7.25)	< .001
DR0405-DR0403	53	2.13 (1.28-3.53)	.003
(DR1403-DQ0301)-(DR1401-DQ0502)	19	2.81 (1.44-5.51)	.002
DP0301-DP0501	49	2.41 (1.49-3.89)	< .001
DP0501-DP0901	71	2.03 (1.30-3.16)	.002

Analysis method is the same as in Table 1. We surveyed specific linked mismatches between nonpermissive mismatches elucidated. As a result, obvious specific linked mismatches exist only between DRB1*1403- DRB1*1401 and DQB1*0301- DQB1*0502. Therefore, we could not evaluate which mismatch combination impacted aGVHD, and we considered this linked mismatch did so. On the other hand, because other nonpermissive mismatch combinations had no specific link with the others, we judged other than DRB1*1403- DRB1*1401 and DQB1*0301- DQB1*0502 nonpermissive mismatches solely impacted aGVHD. (DR1403-DQ0301)-(DR1401-DQ0502) linked mismatch meant that the donor has HLA-DRB1*1403-HLADQB1*0301 and the recipient has HLA-DRB1*1401-HLADQB1*0502.

HR indicates hazard ratio; CI, confidence interval.

group; (3) 1 nonpermissive mismatch (with or without mismatches other than nonpermissive mismatches) group; and (4) 2 or more nonpermissive mismatches (with or without mismatches other than nonpermissive mismatches) group, and analyzed for association with severe aGVHD. This analysis excluded pairs with 2 locus mismatches in the same locus. Patient characteristics according to the number of nonpermissive mismatches are shown in Table 3. The curve of cumulative incidence of severe aGVHD is shown in Figure 1A. Multivariable analysis revealed that severe aGVHD occurred with almost equal frequency between the full match group and zero nonpermissive mismatch group, and was significantly associated with the number of nonpermissive mismatches (Table 4). Relative risk of significant factor for aGVHD and OS is shown in Table S8. In terms of the mortality due to aGVHD according to the number of nonpermissive mismatches, one nonpermissive mismatch group and 2 or more nonpermissive mismatch groups showed higher mortality (19.7% and 15.8%, respectively) than full match group and zero nonpermissive mismatch group (8.5% and 11.4%, respectively).

Impact of positions and types of amino acid substitutions of HLA molecules for severe aGVHD

One specific amino acid substitution at position 9 in HLA-A molecule and 6 specific amino acid substitutions at positions 9, 77, 80, 99, 116, and 156 in HLA-C molecule were significant risk factors for severe aGVHD: Tyr9A-Phe9A (HR: 1.66; CI: 1.19-3.32), Tyr9C-Ser9C (HR: 1.66; CI: 1.23-2.25), Asn77C-Ser77C (HR: 1.87; CI: 1.46-2.39), Lys80C-Asn80C (HR: 1.87; CI: 1.46-2.39), Tyr99C-Phe99C (HR: 1.64; CI: 1.21-2.22), Leu116C-Ser116C (HR: 3.40; CI: 2.20-5.25), and Arg156C-Leu156C (HR: 1.48; CI: 1.15-1.90) (Table 5). The amplitude of hydropathy scales were 4.1, 0.5, 2.7, 0.4, 4.1, 4.6, and 8.3, respectively. Although all

From www.bloodjournal.org at AICHI CNCR CTR on March 24, 2008. For personal use only.

Table 3. Patient characteristics according to number of nonpermissive mismatches

Group	Total	Full match	Zero nonpermissive mismatch	One nonpermissive mismatch	Two or more nonpermissive mismatches
Total	4050	712	2670	602	66
Patient age, median y	30	32	30	29	29
Sex, donor/patient, no. patients					
Male/male	1673	312	1096	237	28
Male/female	785	134	518	119	14
Female/male	769	115	524	117	13
Female/female	823	151	532	129	11
Disease, no. patients					
ALL	981	162	668	139	12
ANLL	1075	196	698	158	23
CML	703	119	453	115	16
Hereditary disease	85	14	56	15	0
MDS	476	91	304	72	9
Malignant lymphoma	349	69	229	48	3
Multiple myeloma	42	8	29	4	1
Severe aplastic anemia	247	33	175	37	2
Other disease	92	20	58	14	0
Risk of leukemia relapse,* no. patients					
Standard risk	1308	249	857	181	21
High risk	1451	228	962	231	30
Diseases other than leukemia	1291	235	851	190	15
GVHD prophylaxis, no. patients					
Cyclosporin-based	2198	402	1444	319	33
Tacrolimus-based	1852	310	1226	283	33
ATG, no. patients					
ATG	323	48	215	53	7
Non-ATG	3727	664	2455	549	59
Preconditioning, no. patients					
TBI regimen	3117	539	2071	449	58
Non-TBI regimen	933	173	599	153	8

ALL indicates acute lymphoblastic leukemia; ANLL, acute non-lymphoblastic leukemia; CML, chronic myeloid leukemia; MDS, myelodysplastic syndrome; and TBI, total body irradiation.

*Standard risk for leukemia relapse was defined as the status of the 1st CR of AML and ALL and the 1st CP of CML at transplant, while high risk was defined as a more advanced status than standard risk in AML, ALL, and CML, and diseases other than leukemia was defined as other than ALL, ANLL, and CML.

amino acid positions substituted in each HLA locus were analyzed, amino acid substitutions of any other HLA-A and -C positions were not significant risk factors. As for HLA-B, DRB1, DQB1, and DPB1, there was no significant association between the positions of amino acid substitution and severe aGVHD. Impact for OS about positions and types of amino acid substitutions that were significant risk factors for aGVHD was shown in Table S9.

Discussion

Extensive recent research has accumulated evidence of the role of each HLA locus mismatch on clinical outcome for UR-HSCT.[3-9] Our next concern is identifying the combinations of HLA allele mismatch and the positions of amino acid substitution of the HLA molecules responsible for aGVHD. In the present study, multivariable analysis revealed that 15 combinations of HLA allele mismatch and 1 HLA-DRB1-DQB1 haplotype mismatch significantly increase the occurrence of severe aGVHD (Table 2), and most of them increased the mortality rate after transplantation (data not shown). Thus, these mismatch combinations of HLA allele might be called nonpermissive clinically. We speculated that the effect of HLA locus mismatch was a reflection and summation of these HLA allele mismatch combinations. Discrepancies of responsible HLA locus for aGVHD between ethnically diverse transplantations might be explained by the proportions of nonpermissive mismatch combinations in each HLA locus. The same study in other populations would be needed to clarify this question as well as the severity of aGVHD. Interestingly, the full match group and zero nonpermissive mismatch group showed an almost equal occurrence of severe aGVHD, though pairs in zero nonpermissive mismatch group had one or more mismatches other than nonpermissive mismatches. And HR was elevated with the increase in the number of nonpermissive mismatches (Figure 1A; Table 4), while the number of nonpermissive mismatches also had a significant effect on OS after transplantation (Figure 1B; Table 4). These findings indicated at least that nonpermissive mismatches should be avoided in donor selection for UR-HSCT, and that the order of donor selection based on this nonpermissive mismatch would be useful, instead of that based on HLA locus mismatch. We also speculated that there are permissive mismatches in mismatches other than nonpermissive mismatches. It is therefore an important task in the future to identify permissive mismatches for partially HLA-matched donor selection. On the other hand, we do not deny the possibility that some mismatch combinations not classified as nonpermissive may actually be potential nonpermissive ones. Misclassification might happen because of insufficient statistical power due to the relatively small number of subjects in subcategories.

At present, there have been only a few reports indicating that the transplant-related immunologic reactions and clinical outcomes were caused by the HLA allele mismatch combinations. Macdonald

From www.bloodjournal.org at AICHI CNCR CTR on March 24, 2008. For personal use only.

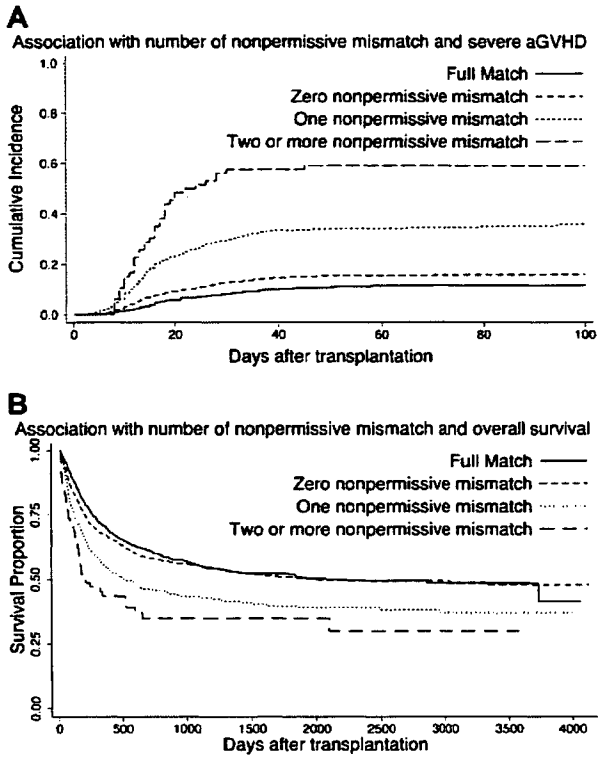

Figure 1. Impact of number of nonpermissive mismatches on severe aGVHD and overall survival. (A) Cumulative incidence of severe aGVHD according to number of nonpermissive mismatches. — indicates full match (in HLA-A, -B, -C, -DRB1, -DQB1, and -DPB1) group; ——, zero nonpermissive mismatch (with mismatches other than nonpermissive mismatches) group; ····, one nonpermissive mismatch (with or without mismatches other than nonpermissive mismatches) group; and – – –, 2 or more nonpermissive mismatches (with or without mismatches other than nonpermissive mismatches) group. (B) Kaplan-Meier estimates of survival according to number of nonpermissive mismatches. Each group was divided as described for panel A.

et al[24] reported that cytotoxic T lymphocytes (CTLs) discriminate between HLA-B*4402 and HLA-B*4403, and induce strong alloresponses, but the stronger T-cell alloreactivity is observed toward HLA-B*4403 compared with HLA-B*4402 in vitro. Zino et al[10] and Fleischhauer et al[11] attempted to develop an algorithm for prediction of nonpermissive HLA-DPB1 mismatches. The present report is the first to provide far more precise and detailed evidence for numerous HLA allele mismatch combinations for severe aGVHD.

Table 5. Multivariable analysis of impact of amino acid substitution on HLA class I molecules for severe aGVHD

Posisiton and kind of amino acid substitution, donor-recipient	HS	N	Event†	HR (95% CI)	P
HLA-A locus					
Tyr9A-Phe9A	4.1	163	64	1.66 (1.19-2.32)	.003
Asn116A-Asp116A	0	32	15	2.25 (1.26-4.01)	.005*
HLA-C locus					
Tyr9C-Ser9C	0.5	146	59	1.66 (1.23-2.25)	.001
Asn77C-Ser77C	2.7	205	90	1.87 (1.46-2.39)	< .001
Lys80C-Asn80C	0.4	205	90	1.87 (1.46-2.39)	< .001
Tyr99C-Phe99C	4.1	146	59	1.64 (1.21-2.22)	.001
Leu116C-Ser116C	4.6	53	30	3.40 (2.20-5.25)	< .001
Arg156C-Leu156C	8.3	251	88	1.48 (1.15-1.90)	.002

HLA-B, -DRB1, -DQB1 -DPB1 locus had no significant substitutions. The impact of positions and types of amino acid substitution in HLA molecules was evaluated in pairs with HLA one-locus mismatch in HLA-A, -B, -C, -DRB1, -DQB1 and -DPB1 separately. For example, Tyr9A-Phe9A indicated amino acid substitutions of position 9 in HLA-A molecule at which donor had tyrosine and patient phenylalanine. The impacts of positions and kinds of amino acid substitutions in each HLA molecule were evaluated in pairs with HLA one locus mismatch in each HLA locus separately. Pairs which substituted specific amino acid at each position were compared with amino acid matched pairs at that position.

HS indicates hydropathy scale; HR, hazard ratio; CI, confidence interval; Tyr, tyrosine; Phe, phenylalanine; Asn, asparagine; Asp, asparatic acid; Ser, serine; Lys, lysine; Leu, leucine; and Arg, arginine.

*Result of base analysis was significant but result of validating analysis using bootstrap resampling was not. Results of analysis were thus judged not to be statistically significant.

†Measured in number of occurrences of severe acute GVHD.

In this study, substitutions of specific amino acids at positions 9, 77, 80, 99, 116, and 156 were elucidated as a significant risk factor for severe aGVHD. We speculated that the responsibility of positions 77 and 80 in HLA-C for severe aGVHD was associated with ligand matching of NK-cell receptor (KIR2DL). Although the role of KIR2DL in acute GVHD has been controversial,[25] a recent JMDP analysis demonstrated that KIR2DL ligand mismatched pairs in GVH vector induced severe aGVHD in UR-HSCT with T-cell–replete marrow.[9] The ligand of KIR2DL is located at positions 77 and 80, which are completely linked in HLA-C molecule. And almost all pairs in this study with Asn77C-Ser77C and Lys80C-Asn80C substitutions have a KIR2DL mismatch in GVH vector.

Except for positions 77 and 80, which are associated with KIR2DL ligand in HLA-C, positions 9, 99, 116, and 156 were elucidated. Positions 9, 99, and 116 are located in the beta-plated

Table 4. Multivariable analysis of impact of number of nonpermissive mismatches on severe aGVHD and overall survival

			Univariate analysis		Multivariate analysis		Bootstrap (10000)	
	N	Event*	HR (95% CI)	P	HR (95% CI)	P	HR (95% CI)	P
For severe aGVHD								
Full match group	972	129	1.00	NA	1.00	NA	1.00	NA
Zero nonpermissive mismatch group	2446	411	1.21 (0.95-1.54)	.111	1.00 (0.75-1.32)	.996	1.00 (0.74-1.33)	.996
One nonpermissive mismatch group	571	211	2.88 (2.20-3.78)	< .001	2.22 (1.62-3.04)	< .001	2.22 (1.63-3.02)	< .001
Two or more nonpermissive mismatch group	61	36	5.62 (3.77-8.39)	< .001	3.68 (2.33-5.80)	< .001	3.68 (2.33-5.80)	< .001
For overall survival								
Full match group	972	400	1.00	NA	1.00	NA	1.00	NA
Zero nonpermissive mismatch group	2446	1021	1.10 (0.98-1.23)	.091	1.06 (0.94-1.20)	.315	1.06 (0.94-1.20)	.299
One nonpermissive mismatch group	571	309	1.55 (1.34-1.78)	< .001	1.51 (1.30-1.76)	< .001	1.51 (1.29-1.77)	< .001
Two or more nonpermissive mismatch group	61	39	2.12 (1.54-2.90)	< .001	2.25 (1.65-3.08)	< .001	2.25 (1.65-3.08)	< .001

Each group was compared with Full match group. Confounders considered were sex (donor-recipient pairs), patient age (linear), donor age (linear), type of disease, risk of leukemia relapse (standard, highand diseases other than leukemia), GVHD prophylaxis, (CSP vs. FK), ATG (ATG vs. no ATG) and preconditioning (TBI vs. non-TBI).

HR indicates hazard ratio; CI, confidence interval; Boot strap (10000), bootstrap resampling using 10000 bootstrapping.

*For severe aGVHD, "Event" refers to number of occurrences; for overall survival, number of deaths.

From www.bloodjournal.org at AICHI CNCR CTR on March 24, 2008. For personal use only.

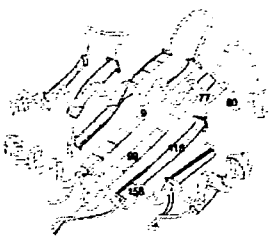

	beta-plate sheet			alpha helix
Position of HLA class I	9	99	116	156
Peptide-binding pocket	B C	A B D	F	D E
Amino acid substitution				
HLA-A	Tyr-Phe		Asn-Asp*	
HLA-C	Tyr-Ser	Tyr-Phe	Leu-Ser	Arg-Leu

Figure 2. Schematic presentation of HLA class I molecule and summary of features of significant amino acid substituted positions. Numbers in schema of HLA molecule indicate substituted amino acid positions that were elucidated as significant risk factor for severe aGVHD. Positions 9, 99, and 116 are located in the beta-plated sheet and positions 77, 80, and 156 in the alpha helix of HLA class I molecule (left). Positions 77 and 80 are associated with KIR2DL ligand in HLA-C molecule. Position 9 constitutes peptide-binding pockets B and C; position 99 constitutes A, B, and D pockets; position 116 constitutes F pocket; and position 156 constitutes D and E pockets (right). For example, Tyr-Phe indicated amino acid substitution at indicated position in HLA molecule at which donor had tyrosine and patient phenylalanine. Tyr indicates tyrosine; Phe, phenylalanine; Asn, asparagine; Asp, asparatic acid; Ser, serine; Lys, lysine; Leu, leucine; and Arg, arginine. *Result of base analysis was significant but result of validating analysis using bootstrap resampling was not. Results of analysis were thus judged not to be statistically significant.

sheet, and position 156 is in the alpha helix of HLA class I molecule (Figure 2).[26,27] Position 9 constitutes peptide-binding pockets B and C, position 99 constitutes A, B, and D pockets, position 116 constitutes F pocket, and position 156 constitutes D and E pockets.[28] As a result, all amino acid positions elucidated in this study were important positions for peptide binding and T-cell recognition, although all substituted positions including positions at which residues are not accessible in the vicinity of peptide binding sites were analyzed.

To our knowledge, amino acid substitutions at position 9 (Tyr9A-Phe9A and Tyr9C-Ser9C) and position 99 (Tyr99C-Phe99C) were newly identified in the present study as responsible for severe aGVHD.

Ferrara et al reported that the amino acid substitution at position 116 in HLA class I molecule increased the risk for aGVHD, although the substituted amino acid was not taken into consideration.[29] In our study, specific amino acid substitution at position 116 had a significant effect in HLA-C (Leu116C-Ser116C) and a marginal effect in HLA-A (Asn116A-Asp116A) for severe aGVHD (Table 5).

Position 156 of HLA molecule was certified to modify T-cell alloreactivity in vitro in HLA-A2,[30-32] HLA-B35,[33] and HLA-B44.[24] For example, in contrast to Asp156B in HLA-B*4402, the nonpolar nature of substituted Leu156B in HLA-B*4403 lost many interactions such as hydrogen bonds and van der Waals interactions with the other amino acid residues that constructed binding pockets. As a result, this substitution made the significant conformation change for alloreactivity.[24] In the HLA-B*3501 and HLA-B*3508 combination, Leu156B in HLA-B*3501 with nonpolar residue was substituted for Asp156B in HLA-B*3508 with polar residue, and induced strong alloreactivity.[33] In our study, the magnitude of the polar change of each substituted amino acid was calculated by "hydropathy scale,"[17] because the influence of this scale on the amino acid interaction was much greater than the influence of the isoelectric point.[34] Specific amino acid substitutions at position 9, 99, 116, and 156, which were not associated with KIR2DL ligand, were found to induce great polar changes except for Tyr9C-Ser9C. Generally speaking, the 3 major physicochemical properties of amino acids that play important roles in protein structure are the hydropathy scale, isoelectric point, and molecular weight, and molecular weight is reflected in the size of amino acids.[34] Indeed, although tyrosine and serine in Tyr9C-Ser9C show few differences in hydropathy scale and isoelectric point, their molecular weights are quite different and may well induce an important conformation change in the HLA molecule. Thus, the change in the conformation by the polar change of the HLA molecule might be one of the mechanisms inducing alloreactivity. These data serve to clarify the mechanisms of aGVHD based on the HLA molecule.

The analysis of HLA-B, -DRB1, -DPB1, and -DQB1 mismatch for the substitution of amino acid elucidated no responsible position for severe aGVHD, and the analysis of HLA-A elucidated only one position. We speculate that the reason for the above result in HLA class I was that in this population there were fewer HLA-mismatched pairs in HLA-A and -B than in HLA-C. Although the findings are due mainly to the HLA-C molecule, specific amino acid substitution at positions 9, 99, 116, and 156 on the HLA class I molecule may induce strong alloreactivity because the structures of HLA class I molecules are quite similar.[29] Indeed, position 9 is selected in HLA-A and -C concurrently, and position 116 had a significant effect on HLA-C and a marginal effect on HLA-A (Figure 2). In HLA class II, we speculated that the molecular base of aGVHD caused by the HLA class II mismatch might be different from that in HLA class I.

In conclusion, we clarified nonpermissive mismatch combinations of all major 6 HLA loci. These data would be beneficial for the selection of suitable donors and international donor exchange for UR-HSCT. Furthermore, we identified the positions and types of amino acid substitutions responsible for severe aGVHD and presented speculations for alloreactivity on the basis of the conformation change of the HLA molecule. These findings provide evidence to elucidate the mechanism of aGVHD on the basis of the HLA molecule.

Acknowledgments

This study was supported in part by Health and Labor Science Research Grant from Ministry of Health, Labor and Welfare of Japan (Research on Human Genome, Tissue Engineering), Grant-in-Aid B from the Japan Society for the Promotion of Science, and a Grant from Third-Term Comprehensive Control Research for Cancer from the Ministry of Health, Labor and Welfare, Japan.

We thank the staff members of the transplant center, donor centers, and JMDP office for their generous cooperation; Ms Ryouko Yamauchi for the data management; and Dr Toshitada Takahashi and Dr Setsuko Kawase for their expert technical assistance.

Authorship

Contribution: T.S., Y.M., T.K., T.J., and Y.K. participated in the conception of this study; K.K., H.I., and H.S. performed the execution for histocompatibility; Y.M. and S.K. performed the execution for transplantation; T.K. and K.M. performed statistical

From www.bloodjournal.org at AICHI CNCR CTR on March 24, 2008. For personal use only.

data analysis; T.K. and Y.M. wrote the paper; all authors checked the final version of the paper.

A complete list of the institutions participating and registering patients through the Japan Marrow Donor Program for the present study is available on the *Blood* website; see the Supplemental Appendix link at the top of the online article.

Conflict-of-interest disclosure: The authors declare no competing financial interests.

Correspondence: Yasuo Morishima, Department of Hematology and Cell Therapy, Aichi Cancer Center, 1-1 Kanokoden chikusa-ku Nagoya 464-8681, Japan; e-mail: ymorisim@aichi-cc.jp.

References

1. Kernan NA, Bartsch G, Ash RC, et al. Analysis of 462 transplantations from unrelated donors facilitated by the National Marrow Donor Program. N Engl J Med. 1993;328:593-602.
2. Kodera Y, Morishima Y, Kato S, et al. Analysis of 500 bone marrow transplants from unrelated donors (UR-BMT) facilitated by the Japan Marrow Donor Program: confirmation of UR-BMT as a standard therapy for patients with leukemia and aplastic anemia. Bone Marrow Transplant. 1999; 24:995-1003.
3. Petersdorf EW, Gooley TA, Anasetti C, et al. Optimizing outcome after unrelated marrow transplantation by comprehensive matching of HLA class I and II alleles in the donor and recipient. Blood. 1998;92:3515-3520.
4. Sasazuki T, Juji T, Morishima Y, et al. Effect of matching of class I HLA alleles on clinical outcome after transplantation of hematopoietic stem cells from an unrelated donor: Japan Marrow Donor Program. N Engl J Med. 1998;339:1177-1185.
5. Morishima Y, Sasazuki T, Inoko H, et al. The clinical significance of human leukocyte antigen (HLA) allele compatibility in patients receiving a marrow transplant from serologically HLA-A, HLA-B, and HLA-DR matched unrelated donors. Blood. 2002;99:4200-4206.
6. Flomenberg N, Baxter-Lowe LA, Confer D, et al. Impact of HLA class I and class II high-resolution matching on outcomes of unrelated donor bone marrow transplantation: HLA-C mismatching is associated with a strong adverse effect on transplantation outcome. Blood. 2004;104:1923-1930.
7. Petersdorf EW, Kollman C, Hurley CK, et al. Effect of HLA class II gene disparity on clinical outcome in unrelated donor hematopoietic cell transplantation for chronic myeloid leukemia: the US National Marrow Donor Program Experience. Blood. 2001;98:2922-2929.
8. Davies SM, Kollman C, Anasetti C, et al. Engraftment and survival after unrelated-donor bone marrow transplantation: a report from the national marrow donor program. Blood. 2000;96:4096-4102.
9. Morishima Y, Yabe T, Matsuo K, et al. Effects of HLA allele and killer immunoglobulin-like receptor ligand matching on clinical outcome in leukemia patients undergoing transplantation with T-cell-replete marrow from an unrelated donor. Biol Blood Marrow Transplant. 2007;13:315-328.
10. Zino E, Frumento G, Marktel S, et al. A T-cell epitope encoded by a subset of HLA-DPB1 alleles determines nonpermissive mismatches for hematologic stem cell transplantation. Blood. 2004;103:1417-1424.
11. Fleischhauer K, Locatelli F, Zecca M, et al. Graft rejection after unrelated donor hematopoietic stem cell transplantation for thalassemia is associated with nonpermissive HLA-DPB1 disparity in host-versus-graft direction. Blood. 2006;107: 2984-2992.
12. Allele Frequencies Database: USA Caucasian Bethesda, USA Olmstead County Minesota. Available at: http://www.allelefrequencies.net. Accessed May 1, 2007.
13. Przepiorka D, Weisdorf D, Martin P, et al. 1994 Consensus Conference on Acute GVHD Grading. Bone Marrow Transplant. 1995;15:825-828.
14. IMGT/HLA Sequence Database. Available at: http://www.ebi.ac.uk/imgt/hla/. Accessed February 1, 2007.
15. Socie G. Graft-versus-host disease–from the bench to the bedside? N Engl J Med. 2005;353: 1396-1397.
16. Hansen JA, Gooley TA, Martin PJ, et al. Bone marrow transplants from unrelated donors for patients with chronic myeloid leukemia. N Engl J Med. 1998;338:962-968.
17. Kyte J, Doolittle RF. A simple method for displaying the hydropathic character of a protein. J Mol Biol. 1982;157:105-132.
18. Gooley TA, Leisenring W, Crowley J, Storer BE. Estimation of failure probabilities in the presence of competing risks: new representations of old estimators. Stat Med. 1999;18:695-706.
19. Coviello V, Boffess M. Cumulative incidence estimation in the presence of compiting risks. Stata J. 2004;4:103-112.
20. Cox DR. Regression models and life-tables. J R Stat Soc (B). 1972;34:187-220.
21. Peduzzi P, Concato J, Kemper E, Holford TR, Feinstein AR. A simulation study of the number of events per variable in logistic regression analysis. J Clin Epidemiol. 1996;49:1373-1379.
22. Efron B. Bootstrap methods: another look at the jackknife. Ann Stat. 1979;7:1-26.
23. Manly BFJ. Randomization, Bootstrap and Monte Carlo Methods in Biology. London, United Kingdom: Chapman and Hall; 1997.
24. Macdonald WA, Purcell AW, Mifsud NA, et al. A naturally selected dimorphism within the HLA-B44 supertype alters class I structure, peptide repertoire, and T cell recognition. J Exp Med. 2003;198:679-691.
25. Parham P. MHC class I molecules and KIRs in human history, health and survival. Nat Rev Immunol. 2005;5:201-214.
26. Bjorkman PJ, Saper MA, Samraoui B, Bennett WS, Strominger JL, Wiley DC. Structure of the human class I histocompatibility antigen, HLA-A2. Nature. 1987;329:506-512.
27. Petersdorf EW, Hansen JA, Martin PJ, et al. Major-histocompatibility-complex class I alleles and antigens in hematopoietic-cell transplantation. N Engl J Med. 2001;345:1794-1800.
28. Steven GE, Peter P, Linda DB. The HLA Facts Book. London, United Kingdom: Academic Press; 2000.
29. Ferrara GB, Bacigalupo A, Lamparelli T, et al. Bone marrow transplantation from unrelated donors: the impact of mismatches with substitutions at position 116 of the human leukocyte antigen class I heavy chain. Blood. 2001;98:3150-3155.
30. Hogan KT, Clayberger C, Bernhard EJ, et al. Identification by site-directed mutagenesis of amino acid residues contributing to serologic and CTL-defined epitope differences between HLA-A2.1 and HLA-A2.3. J Immunol. 1988;141:2519-2525.
31. Mattson DH, Shimojo N, Cowan EP, et al. Differential effects of amino acid substitutions in the beta-sheet floor and alpha-2 helix of HLA-A2 on recognition by alloreactive viral peptide-specific cytotoxic T lymphocytes. J Immunol. 1989;143: 1101-1107.
32. Shimojo N, Cowan EP, Engelhard VH, Maloy WL, Coligan JE, Biddison WE. A single amino acid substitution in HLA-A2 can alter the selection of the cytotoxic T lymphocyte repertoire that responds to influenza virus matrix peptide 55-73. J Immunol. 1989;143:558-564.
33. Tynan FE, Elhassen D, Purcell AW, et al. The immunogenicity of a viral cytotoxic T cell epitope is controlled by its MHC-bound conformation. J Exp Med. 2005;202:1249-1260.
34. Biro JC. Amino acid size, charge, hydropathy indices and matrices for protein structure analysis. http://www.tbiomed.com/content/pdf/1742-4682-3-15.pdf. Accessed February 1, 2007.

Age-Related EBV-Associated B-Cell Lymphoproliferative Disorders Constitute a Distinct Clinicopathologic Group: A Study of 96 Patients

Takashi Oyama,[1] Kazuhito Yamamoto,[2] Naoko Asano,[3] Aya Oshiro,[3] Ritsuro Suzuki,[4] Yoshitoyo Kagami,[2] Yasuo Morishima,[2] Kengo Takeuchi,[7] Toshiyuki Izumo,[9] Shigeo Mori,[8] Koichi Ohshima,[10] Junji Suzumiya,[11] Naoya Nakamura,[12] Masafumi Abe,[12] Koichi Ichimura,[13] Yumiko Sato,[13] Tadashi Yoshino,[13] Tomoki Naoe,[5] Yoshie Shimoyama,[6] Yoshikazu Kamiya,[1] Tomohiro Kinoshita,[5] and Shigeo Nakamura[6]

Abstract **Purpose:** We have recently reported EBV+ B-cell lymphoproliferative disorders (LPD) occurring predominantly in elderly patients, which shared features of EBV+ B-cell neoplasms arising in the immunologically deteriorated patients despite no predisposing immunodeficiency and were named as senile or age-related EBV+ B-cell LPDs. To further characterize this disease, age-related EBV+ B-cell LPDs were compared with EBV-negative diffuse large B-cell lymphomas (DLBCL).

Experimental Design: Among 1,792 large B-cell LPD cases, 96 EBV+ cases with available clinical data set were enrolled for the present study. For the control group, 107 patients aged over 40 years with EBV-negative DLBCL were selected. We compared clinicopathologic data between two groups and determined prognostic factors by univariate and multivariate analysis.

Results: Patients with age-related EBV+ B-cell LPDs showed a higher age distribution and aggressive clinical features or parameters than EBV-negative DLBCLs: 44% with performance status >1, 58% with serum lactate dehydrogenase level higher than normal, 49% with B symptoms, and higher involvement of skin and lung. Overall survival was thus significantly inferior in age-related EBV+ group than in DLBCLs. Univariate and multivariate analyses further identified two factors, B symptoms and age older than 70 years, independently predictive for survival. A prognostic model using these two variables well defined three risk groups: low risk (no adverse factors), intermediate risk (one factor), and high risk (two factors).

Conclusions: These findings suggest that age-related EBV+ B-cell LPDs constitute a distinct group, and innovative therapeutic strategies such as EBV-targeted T-cell therapy should be developed for this uncommon disease.

Authors' Affiliations: Departments of [1]Clinical Oncology, [2]Hematology and Cell Therapy, [3]Pathology and Molecular Diagnostics, and [4]Division of Molecular Medicine, Aichi Cancer Center, [5]Department of Hematology, Nagoya University Graduate School of Medicine, and [6]Department of Pathology and Clinical Laboratories, Nagoya University Hospital, Nagoya, Japan; [7]Department of Pathology, The Cancer Institute of the Japanese Foundation for Cancer Research, and [8]Department of Pathology, Teikyo University School of Medicine, Tokyo, Japan; [9]Department of Pathology, Saitama Cancer Center, Saitama, Japan; [10]Department of Pathology, School of Medicine, Kurume University, Kurume, Japan; [11]First Department of Internal Medicine, Fukuoka University School of Medicine, Fukuoka, Japan; [12]First Department of Pathology, Fukushima Medical College, Fukushima, Japan; and [13]Department of Pathology, Okayama University Graduate School of Medicine and Dentistry, Okayama, Japan

Received 11/28/06; revised 5/8/07; accepted 6/21/07.

Grant support: Grant-in-Aid for Scientific Research from the Ministry of Education, Science, Sports, Culture and Technology of Japan and in part by the Health and Labor Science Research Grants.

The costs of publication of this article were defrayed in part by the payment of page charges. This article must therefore be hereby marked *advertisement* in accordance with 18 U.S.C. Section 1734 solely to indicate this fact.

Note: Supplementary data for this article are available at Clinical Cancer Research Online (http://clincancerres.aacrjournals.org/).

Requests for reprints: Kazuhito Yamamoto, Department of Hematology and Cell Therapy, Aichi Cancer Center, 1-1 Kanokoden, Chikusa-ku, Nagoya 464-8681, Japan. Phone: 81-52-762-6111; Fax: 81-52-764-2941; E-mail: kyamamoto@aichi-cc.jp.

©2007 American Association for Cancer Research.

doi:10.1158/1078-0432.CCR-06-2823

Diffuse large B-cell lymphoma (DLBCL) is the largest category of aggressive lymphomas and regarded as a heterogeneous group of lymphomas in terms of clinicopathologic profiles and biological properties (1). Recent advance in the lymphoma research shed the light on the distinct subgroups such as *de novo* CD5+ DLBCL (2), intravascular large B-cell lymphoma (Asian variant; ref. 3), primary effusion lymphoma (4), and pyothorax-associated lymphoma (5) under the nosologic term of DLBCL. In addition, we have recently identified a series of elderly patients of EBV+ B-cell lymphoproliferative disorders (LPD) and/or large-cell lymphomas without predisposing immunodeficiencies and named those senile or age-related EBV+ B-LPDs (6).

EBV is a ubiquitous γ-herpesvirus that infects more than 90% of worldwide adult population (7, 8). In contrast to its high prevalence, EBV is also well recognized as an apparent oncogenic agent (9). It transforms B cells into lymphoblastoid cell lines *in vitro*, and many human cancers, including Burkitt lymphoma (BL) (10), Hodgkin lymphoma (7), immunodeficiency-associated LPDs (11), and a part of diffuse large B-cell lymphoma (12), have close relation with EBV. Although the precise mechanism is not fully clarified, it is widely accepted that the T cell plays a crucial role for the suppression of EBV-associated oncogenesis (7). In fact, the use of strong

immunosuppressive agents in organ transplantation settings such as tacrolimus or cyclosporin A, or HIV infection, sometimes causes EBV-positive B-cell LPDs (13, 14). Four clinical settings of immunodeficiency associated with an increased incidence of lymphoma and other LPDs are recognized by the WHO classification: (*a*) primary immunodeficiency syndromes and other primary immune disorders; (*b*) infection by the HIV; (*c*) iatrogenic immunosuppression in patients who have received solid organ or bone marrow allografts; and (*d*) iatrogenic immunosuppression associated with methotrexate treatment, most commonly in patients with autoimmune disease (15).

We have highlighted the over-profile of senile EBV+ B-cell LPDs appearing analogous in many respects to that of immunodeficiency-associated B-cell LPDs, which were exemplified by a marked propensity to involve extranodal sites and a morphologic spectrum ranging from the precursor polymorphous proliferation of lymphoid cells to diverse types of lymphomas, although no evidence of underlying immunodeficiency was found (6). Therefore, it is speculated that this disease is related to an immunologic deterioration derived from the aging process, i.e., senescence in immunity. However, the detailed clinicopathlogic features and follow-up information of age-related EBV+ B-cell LPDs remain limited because of an inclusion of a small number of patients and the lack of the comparison with EBV-negative DLBCL. To address these issues further, we retrospectively assessed the clinicopathologic features of 96 cases with age-related EBV+ B-cell LPDs as a collaborative study.

Materials and Methods

Diagnosis. The diagnosis of age-related EBV-associated B-cell LPDs was made when more than 50% of the proliferating, often neoplastic-appearing cells showed both of the expression of one or more pan-B-cell antigens (CD20/CD79a) and/or light-chain restriction and positive signal for *in situ* hybridization using EBV-encoded small nuclear early region (EBER) oligonucleotides on paraffin section (Fig. 1) for patients more than 40 years of age without predisposing immunodeficiency such as HIV infection or past history of immunosuppressive agents (6) The cases <40 years old were excluded because we could not deny the possibility that they may be associated with any primary immune disorder or chronic active EBV infection (16, 17). In addition, pyothorax-associated lymphoma and EBV-associated lymphomas of T- or natural killer-cell phenotype were excluded from the present series because they were considered to constitute distinct clinicopathologic groups (5, 18). In particular, attention was given to the differential diagnoses of peripheral T-cell lymphoma with Reed-Sternberg-like cells of B-cell or angioimmunoblastic T-cell lymphoma with proliferation of large B cells (19). Only well-documented cases that had paraffin sections available for immunohistochemistry were included in this study. Each case was reviewed by five pathologists (authors K.T., K.O., N.N. T.Y., and S.N.) to confirm the diagnosis and immunophenotype. Among 149 cases fulfilling these criteria (Supplementary Table S1), 96 cases with available clinical data set were enrolled for the present study, including the 22 cases of senile EBV+ B-cell LPDs previously reported by us (6). For the control group, 107 patients aged over 40 years with EBV-negative DLBCL were selected from malignant lymphoma cases treated consecutively at Aichi Cancer Center between 1993 and 2000. This study was done by following the Ethical Guidelines for Clinical Studies and the Ethical Guideline for Epidemiological Research in Japan. The Institutional Review Board of the Aichi Cancer Center and the other institutes involved approved this study.

Histopathology. Tissue samples were fixed in 10% formalin and embedded in paraffin. Sections (5 μm thick) were stained with H&E, Elastica-van Gieson, silver impregnation, periodic acid-Schiff, May-Gruenwald-Giemsa, and methyl green-pyronine staining.

Immunohistochemistry. Immunoperoxidase studies were done on formalin-fixed paraffin sections with the avidin-biotin peroxidase complex method. A panel of monoclonal antibodies against human immunoglobulin light and heavy chains, CD3, CD8, UCHL-1/CD45RO, L26/CD20, Ber-H2/CD30, CD79a, latent membrane protein-1 (LMP-1), EBV-encoded nuclear antigen-2 (EBNA2; DAKO); CD2, CD4, CD5, CD56 (Novocastra Laboratories); LeuM1/CD15, Leu7/CD57

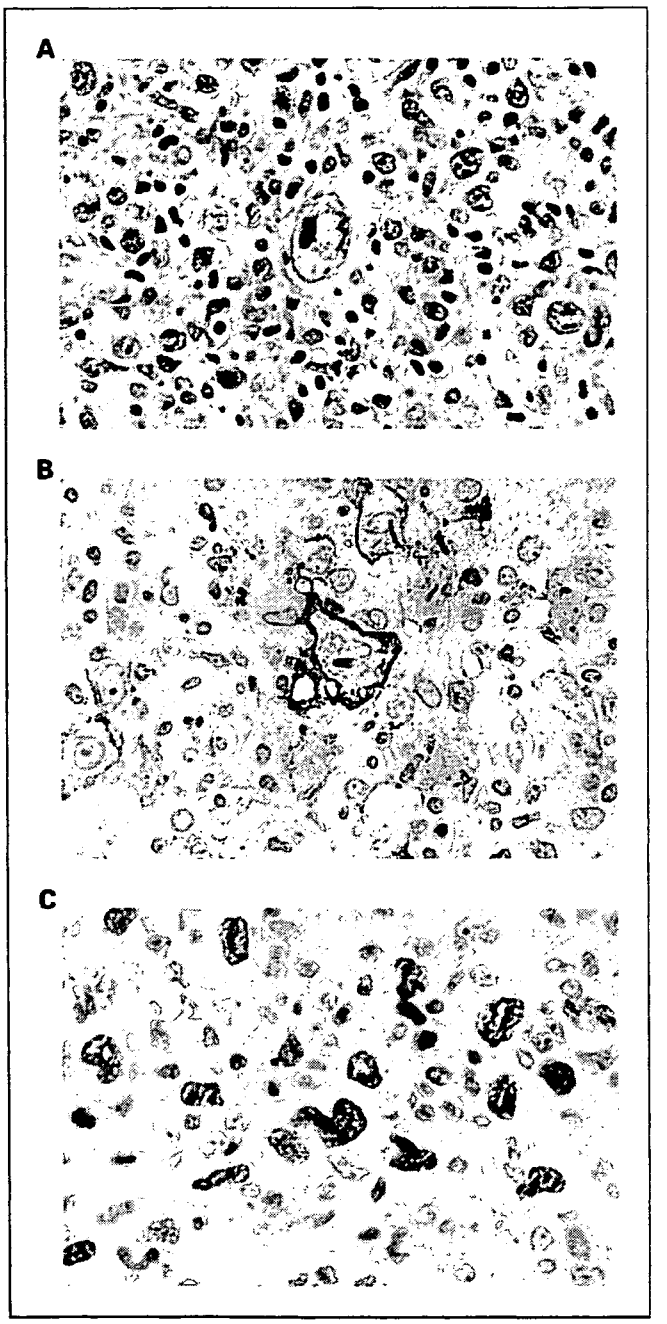

Fig. 1. Senile EBV-associated B-cell LPD, polymorphic subtype, arising in a 62-year-old male. The lesion reveals scattered distribution of Hodgkin and Reed-Sternberg – like giant cells (*A*, ×150), which are positive for CD20 (*B*, ×125). These large cells showed the expression of EBNA2 (*C*, ×125) in addition to the positive signals for EBV-encoded small RNAs (EBERs) *in situ* hybridization, indicating latency III status.

Table 1. Patient characteristics at diagnosis of age-related EBV-positive B-LPDs and EBV-negative DLBCL

Variable	Age-related EBV-positive LPD (n = 96)	EBV-negative DLBCL (n = 107)	P
Sex (male/female)	56/40 (1.4)	54/53 (1.02)	0.26
Age, median (range), y	71 (45-92)	62 (41-85)	<0.0001
	Number of cases (%)	**Number of cases (%)**	
Older than 60	79 (82%)	56 (52%)	<0.0001
ECOG PS 2-4	36 (44%)	18 (17%)	<0.0001
B-symptoms, presence	38 (49%)	18 (20%)	<0.0001
LDH level high	47 (58%)	46 (43%)	0.041
Ann Arbor stage III/IV	48 (58%)	49 (46%)	0.10
Extranodal involvement (>1 site)	28 (33%)	30 (28%)	0.43
Extranodal sites	n = 93	n = 107	
Skin	12 (13%)	5 (5%)	0.037
Lung	8 (9%)	3 (3%)	0.073
Pleural effusion	8 (9%)	5 (5%)	0.26
Stomach	8 (9%)	14 (13%)	0.31
Tonsil	7 (8%)	20 (19%)	0.021
Breast	0 (0%)	7 (7%)	0.012
IPI, High intermediate/high	43 (54%)	39 (37%)	0.017
Anti-EBV antibody titer category,*	18 (67%)	23 (24%)	<0.0001
Treatment			<0.0001
None or radiation only	9 (12%)	1 (1%)	
Ctx without anthracycline	7 (9%)	2 (2%)	
Ctx with anthracycline	62 (79%)	104 (97%)	
Response, in cases underwent Ctx with anthracycline			<0.0001
CR	37 (66%)	93 (91%)	
PR	8 (14%)	8 (8%)	
SD or PD	11 (20%)	1 (1%)	

Abbreviations: PS, performance status; LDH, lactate dehydrogenase; IPI, International Prognostic Index; Ctx, chemotherapy; CR indicates complete response; PR, partial response; SD, stable disease; PD, progressive disease.
*Cases were determined as having abnormal serum anti-EBV antibody titer if anti-EBV viral capsid antigen antibody was 640-fold or higher, or anti-EBV nuclear antigen antibody was negative.

(Becton Dickinson); TIA-1 (Coulter Immunology); and granzyme B (Monosan) were used. All antibodies were applied after antigen retrieval following microwave oven heating treatment.

In situ *hybridization study.* The presence or absence of EBV small RNAs was assessed by means of *in situ* hybridization using EBER oligonucleotides and done on formalin-fixed paraffin embedded sections. Briefly, a DAKO hybridization kit was used with a cocktail of FITC-labeled EBER oligonucleotides (one oligonucleotide corresponding to EBER1 and one to EBER2, both 30 bases long; DAKO A/S code Y 017). Hybridization products were detected with mouse monoclonal anti-FITC (DAKO M878) and a Vectastain ABC Kit (Vector). RNase A or DNase I pretreatment was used for the negative controls and EBER-positive Hodgkin's disease specimens for positive controls.

Statistical analysis. Variables related to patients, treatment, and disease were compared among the two groups with the use of the χ^2 test or Fisher's exact test for categorical variables and the Mann-Whitney U test for continuous variables. The probability of survival was calculated with the use of the Kaplan-Meier estimator, and the log-rank test was used for comparisons. Univariate and multivariate analyses were done with the Cox proportional hazard regression model. All P values are two sided, with a type I error rate fixed at 0.05. Statistical analyses were done with the STATA version 9.

Results

Case selection. From the files of six collaborating institutions, during the period from January 1990 to December 2004, the positive signals for B-cell [pan-B-cell antigens (CD20/CD79a) and/or light-chain restriction] and EBV were detected on more than 50% of cells in 243 (14%) of 1,792 large B-cell LPD cases, mainly consisting of DLBCL, by EBERs *in situ* hybridization. They contained HIV-associated lymphomas (n = 17), autoimmune disease-associated LPDs (n = 10), secondary lymphoma with prior chemotherapy (n = 7), post-transplant LPDs (n = 10), pyothorax-associated lymphoma (n = 30), BL (n = 13), and cases without any documentation for predisposing immunodeficiency (n = 156; Supplementary Table S1). EBV was detected in 10% of HIV-negative patients with BL in this study, which was comparable to the reported frequency in nonendemic BL (20). A bimodal age distribution with an incidence peak in the 10- to 19-year range and a second peak in older adult aged 70 to 79 was evident for EBV-positive B-cell LPD patients without predisposing immunodeficiency (Supplementary Fig. S1*A*). The positive percentages of this group for all cases examined became higher in parallel with the elder patient populations (≥40 years), showing the highest peak at ages >90 years (Supplementary Fig. S1*B*).

Patient characteristics for age-related EBV-positive B-cell LPDs and EBV-negative DLBCL. In comparison with EBV-negative DLBCL, patients with age-related EBV-positive B-cell LPDs showed higher age distribution (median, 71 versus 62 years: $P < 0.0001$) and a closer association with aggressive clinical features or parameters: 79 patients older than 60 (82%,

$P < 0.0001$), 36 with performance status (PS) >1 (44%, $P < 0.0001$), 47 with serum lactate dehydrogenase (LDH) level higher than normal (58%, $P = 0.041$), 48 with stage III/IV disease at diagnosis (58%, $P = 0.10$), and 38 with B symptoms (49%, $P < 0.0001$; Table 1). As a result, the International Prognostic Index (IPI) score for patients with age-related EBV-positive B-cell LPDs was significantly higher than that for patients with EBV-negative DLBCL ($P = 0.0017$), with 43 (54%) of the EBV-positive group categorized in the IPI high or high intermediate-risk group. There was no statistical difference between two groups in the incidence of having more than one extranodal site.

At diagnosis, 67% of the cases with age-related EBV-positive B-cell LPDs showed abnormal anti-EBV antibody titer, which was defined if anti-EBV VCA immunoglobulin G (IgG) antibody was 640-fold or higher, or anti-EBNA antibody was negative, as compared with only 24% of cases with DLBCL that showed abnormality ($P < 0.0001$).

Sites of extranodal involvement. In 17 patients (20%) of the current EBV-positive series, the disease was limited to extranodal sites. Twenty-seven patients (31%) had only lymphadenopathies without extranodal involvement, and the remaining 43 (49%) had lymphadenopathies with extranodal involvement. The total incidence of extranodal involvement was similar between age-related EBV-positive B-cell LPDs and EBV-negative DLBCL (69% and 72%, respectively).

The main sites of extranodal involvement in age-related EBV-positive B-cell LPDs was skin ($n = 12$; 13%), lung ($n = 8$; 9%), pleural effusion ($n = 8$; 9%), stomach ($n = 8$; 9%), and tonsil ($n = 7$; 8%) in an order of the incidence (Table 1). A comparison with EBV-positive and EBV-negative groups showed that the incidence of cutaneous involvement was significantly higher in age-related EBV-positive B-cell LPDs than those of EBV-negative DLBCLs ($P = 0.027$, respectively). There is a tendency of difference in lung involvement, but no statistical significance (9% versus 3%, $P = 0.073$). Involvement of breast and tonsil occurred less frequently in age-related EBV-positive B-cell LPDs than in EBV-negative DLBCL ($P = 0.012$ and.021, respectively). There were no significant differences between these two groups in the incidence of involvement in the other extranodal sites (Supplementary Table S2).

Histologic features. Age-related EBV-positive LPDs generally showed a diffuse and polymorphic proliferation of large lymphoid cells with a varing degree of reactive components such as small lymphocytes, plasma cells, histocytes, and epithelioid cells and were sometimes accompanied by necrosis and an angiocentric pattern. These tumor cells were often featured by a broad range of B-cell maturation, containing morphologic centroblasts, immunoblasts, and Hodgkin and Reed-Sternberg (HRS)-like giant cells with distinct nucleoli (Fig. 1*A*). According to the previous report (6), the present series were morphologically divided into two subtypes: large-cell lymphoma (LCL) and polymorphic LPD subtypes. The former ($n = 34$) was characterized by having areas where large lymphoid cells with relatively monomorphic appearance were notably dominant. The remaining 62 cases were simply categorized as polymorphous subtype with the scattered distribution of large cells in the polymorphous composition. The histology was frequently varied from area to area, indicating a continuous spectrum between these two subgroups because several LCL cases had areas of polymorphic LPD in the same or other tissues. In contrast to morphologic divergence, there was no significant difference in any clinical characteristics and immunophenotype between these two groups (Supplementary Table S3).

We detected clonal B-cell population in 10 cases out of 12 cases tested: eight cases by PCR analysis, one case by Southern blot analysis, and one by lambda light-chain restriction. Polyclonal pattern was observed in one case, and no band was detected in the other. As to polymorphic LPDs, the presence of clonal B-cell population was identified in five cases out of seven samples.

Phenotypic features. According to the definition adopted for this study, all patients with age-related EBV-positive B-cell LPDs were positive for EBV and B-cell markers (CD20 and/or CD79a; Fig. 1*B*). Immunohistologic studies for the EBV-latent gene products on paraffin sections showed that LMP1 was positive on the large atypical cells in 67 (94%) out of 71 tested cases. EBNA2 was also detected in the nuclei of 16 (28%) of 57 tested cases (Fig. 1*C*, Supplementary Table S4), indicating latency type III. CD30 was stained more common in age-related EBV-positive B-cell LPDs than in EBV-negative DLBCL (75% versus 13%, $P < 0.0001$). In addition, a comparison of adjacent sections often disclosed an overlapping staining pattern of LMP1 and CD30. There was also a statistically significant difference in the incidence of CD10 expression (18% and 38%, respectively. $P = 0.015$), but not others (CD19, CD20, or CD79a) between age-related EBV-positive B-cell LPDs and DLBCLs (Supplementary Table S4).

Response to treatment and Kaplan-Meier survival estimates. Treatment of age-related EBV-positive B-cell LPDs consisted of chemotherapeutic regimens containing anthracycline for 62 patients (79%) and without anthracycline for 7 patients (9%; Table 1). A total of 40 (63%) of 64 evaluable patients with age-related EBV-positive B-cell LPDs achieved a complete remission (CR) with initial therapy, and the rest of the 24 cases (38%) failed to have a CR with initial chemotherapy. On the other hand, 95 (91%) of 104 evaluable cases with DLBCL achieved a CR, and only 9 cases (9%) were refractory (PR, SD, or PD) to initial chemotherapy ($P < 0.0001$). This difference, in response to treatment, was still in a significant level when compared in cases who received chemotherapy with anthracycline ($P < 0.0001$, Table 1).

In this study, we observed 57 deaths in 96 cases of age-related EBV-positive B-cell LPDs and 34 deaths in 107 cases of DLBCL. The data on the causes of death were available for 47 cases for age-related EBV-positive B-cell LPDs and 29 for DLBCL. Deaths due to disease progression and complications such as infections were observed in 38 and 9 cases, respectively, in age-related EBV-positive B-cell LPDs, whereas 23 and 6 cases in EBV-DLBCL. The observed differences between two disease groups were not significant ($P = 0.870$). As to the cases of more than 70 years of age, 24 and 5 cases were dead due to disease progression, and seven and one were from complications in age-related EBV-positive B-cell LPDs and in DLBCL, respectively. Even in cases more than 70 years old, the observed differences were not significant ($P = 0.747$).

Unadjusted overall survival curves of both groups were shown in Fig. 2*A*. Age-related EBV-positive B-cell LPDs showed strikingly inferior survival to DLBCLs (median survival time, 24 months versus not reached, respectively;

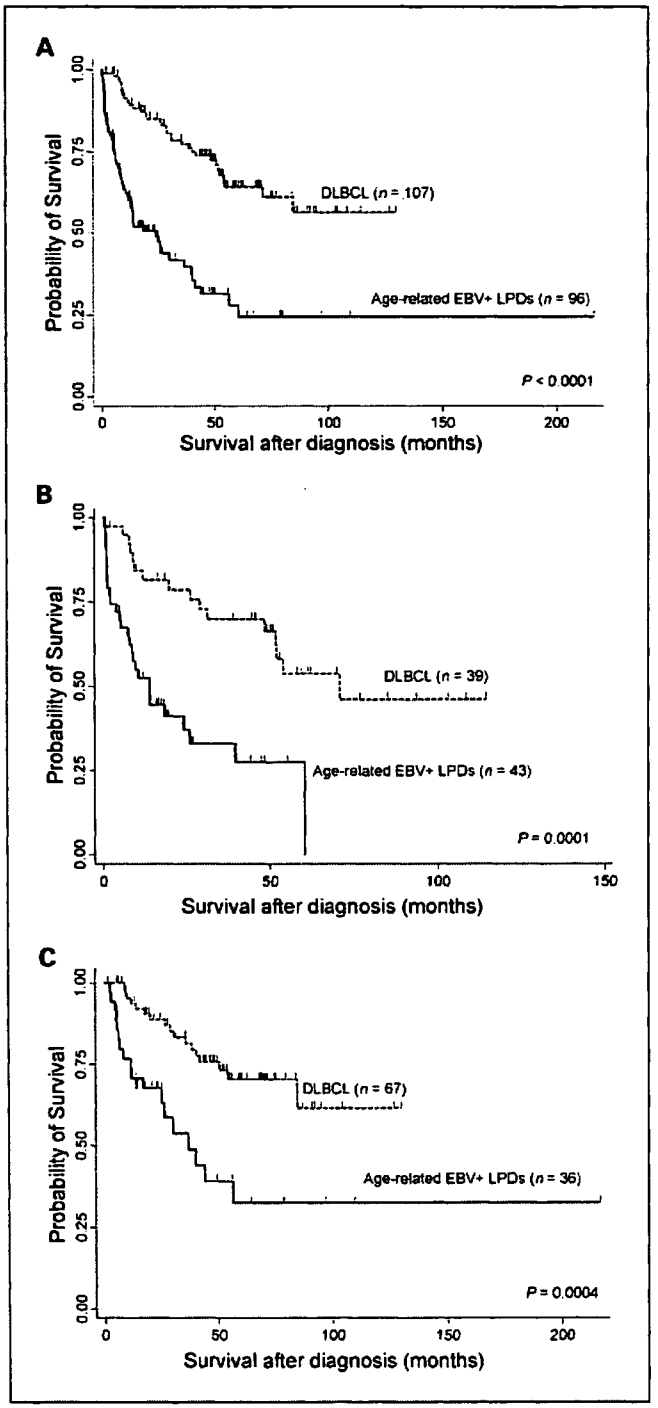

Fig. 2. Overall survival for patients with age-related EBV+ B-cell LPDs and EBV-negative DLBCLs. Age-related EBV+ B-cell LPDs (n = 96) show significantly worse survival than DLBCLs (n = 107) in all patients (A), patients with high-intermediate and high IPI risk (n = 43 and n = 39, respectively; B), and patients with low and low-intermediate IPI risk group (n = 36 and n = 67, respectively; C).

P < 0.0001). A significant difference was still found even when accounting for age (age ≤ 60, 60 < age ≤ 75, or age > 75) by performing the stratified log-rank test (P < 0.0001). Overall survival curves according to IPI are shown in Fig. 2B and C. Survival for age-related EBV-positive B-cell LPDs was significantly inferior to that for DLBCLs in both IPI subgroups. In this series, the IPI failed to separate age-related EBV+ B-cell LPD patients into groups with significantly different survivals (P = 0.1; Fig. 3A).

Univariate and multivariate analysis for survival. Among a total of 203 patients with EBER-positive (age-related EBV-positive B-cell LPDs) and EBV-negative diseases (DLBCLs), univariate Cox analysis identified the following as prognostic factors: age > 60 years, clinical stage, PS, extranodal involvement of more than one site, LDH, IPI, B symptoms, and EBV association (Table 2). Multivariate analysis, including five IPI factors, B symptoms, and EBV association, showed high LDH level, the presence of B-symptoms, and EBV association to be significant factors (Table 2). When multivariate analysis was done for EBV association and IPI categories, both of them were recognized as independent significant prognostic factors (Table 2).

Among patients with age-related EBV+ B-cell LPDs, the clinical parameters associated with reduced survival in univariate analysis are listed in Table 3: age older than 70

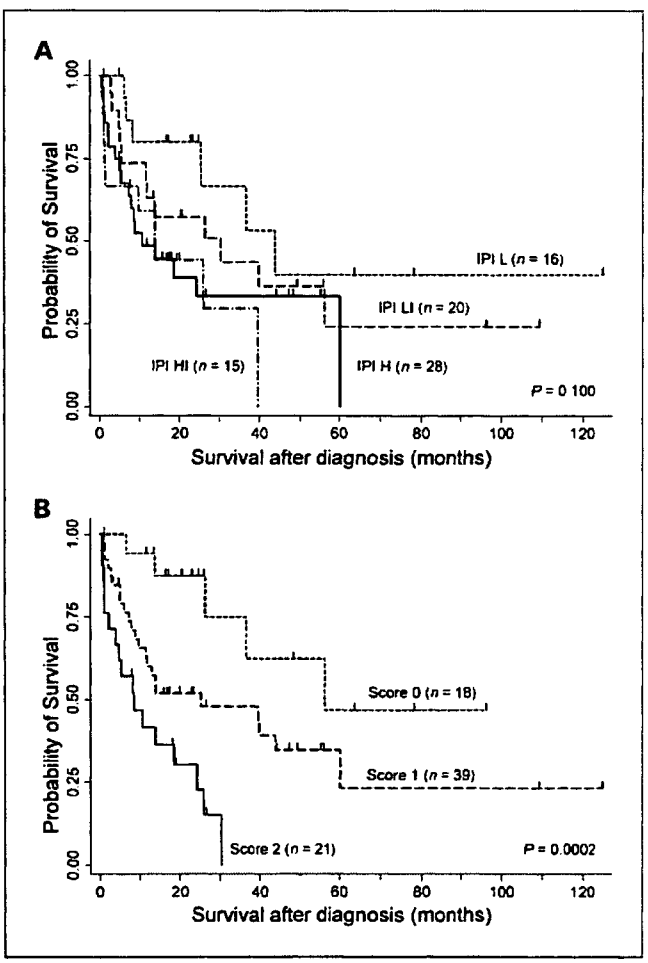

Fig. 3. Overall survival according to IPI (A) and prognostic model based on two simple clinical variables of age older than 70 y and the presence of B symptoms (B) in age-related EBV+ B-cell LPDs. This prognostic model is able to efficiently identify three groups of patients with different outcomes; patients with a score of 0 (*Score 0*, n = 18), no adverse factors; patients with a score of 1 (*Score 1*, n = 39), one factor; and patients with a score of 2 (*Score 2*, n = 21), two factors. Their median survival times were 56.3, 25.2, and 8.5 mo, respectively.